

Learning Asynchronous and Error-prone Longitudinal Data via Functional Calibration

Xinyue Chang

Lilly Corporate Center

Eli Lilly and Company

Indianapolis, IN 46225, USA

CHANG_XINYUE@LILLY.COM

Yehua Li

Department of Statistics

University of California

Riverside, CA 92521, USA

YEHUALI@UCR.EDU

Yi Li

Department of Biostatistics

University of Michigan

Ann Arbor, MI 48109, USA

YILI@UMICH.EDU

Editor: TBD

Abstract

In many longitudinal settings, time-varying covariates may not be measured at the same time as responses and are often prone to measurement error. Naive last-observation-carried-forward methods incur estimation biases, and existing kernel-based methods suffer from slow convergence rates and large variations. To address these challenges, we propose a new functional calibration approach to efficiently learn longitudinal covariate processes based on sparse functional data with measurement error. Our approach, stemming from functional principal component analysis, calibrates the unobserved synchronized covariate values from the observed asynchronous and error-prone covariate values, and is broadly applicable to asynchronous longitudinal regression with time-invariant or time-varying coefficients. For regression with time-invariant coefficients, our estimator is asymptotically unbiased, root-n consistent, and asymptotically normal; for time-varying coefficient models, our estimator has the optimal varying coefficient model convergence rate with inflated asymptotic variance from the calibration. In both cases, our estimators present asymptotic properties superior to the existing methods. The feasibility and usability of the proposed methods are verified by simulations and an application to the Study of Women's Health Across the Nation, a large-scale multi-site longitudinal study on women's health during mid-life.

Keywords: regression calibration, functional principal component analysis, kernel smoothing, measurement error, sparse functional data, varying coefficient model.

1. Introduction

In many decade-long longitudinal studies, participants' health information is repeatedly measured by diverse instruments, such as blood tests, physical examinations, nutritional evaluations and psychological assessments. These tests and assessments usually follow different schedules, and are not synchronized in time. The resulting data structures create an

asynchronous issue where the response variable and covariates are not measured at the same time. For example, in our motivating Study of Women’s Health Across the Nation (SWAN; <https://www.swanstudy.org/>), a multi-site longitudinal study on women’s health during their mid-life years, a total of 3,302 women were followed from 1996 to 2008 to study their physical, biological, psychological, and social changes that occurred during the menopausal transition. These health-related metrics were grouped into physical, hormone, and cardiovascular measurements. Fig 1 shows the measurement times for hormone, physical and cardiovascular measurements for a random sample of SWAN participants. As seen, these measurements were taken following different schedules. During this important transition, of particular interest is the level of the follicle-stimulating hormone (FSH), our response variable. Two important physical and cardiovascular covariates, the body mass index (BMI) and triglycerides (TG), are also repeatedly measured but on different schedules. Another complication as manifested by Fig 2, a spaghetti plot for the longitudinal trajectories of these three variables from a randomly selected participant, is that these asynchronized variables also exhibit short term fluctuations, which need to be modeled as measurement error or nugget effect (Carroll et al., 2006).

A naive last-observation-carried-forward (LOCF) method ignores the dynamics of time-varying covariates, takes the most recent measurement as the current value of the covariate, and performs routine regression analyses. It is known such a method leads to biased and inconsistent estimates of the regression coefficients (Molenberghs et al., 2004). There has been some literature on analyzing incomplete longitudinal data using missing data techniques such as the inverse probability weighting: Robins et al. (1995) assumed the response and time-varying covariates must be missing or present simultaneously; Cook et al. (2004) assumed that the repeated measurements within a subject are complete before the subject dropout from the study. These methods rely on parametric modeling of the missing data mechanism and are not designed for data that are asynchronous by design.

More recently, Cao et al. (2015) and Cao et al. (2016) learned asynchronous longitudinal data under generalized linear models with either time-invariant or time-varying coefficients, by proposing kernel-weighted estimating equation methods to down-weight covariates that are further away in time from the response. These kernel-weighted estimators are consistent and asymptotically normal, but with slow convergence rates. For time-invariant regression models, their estimated regression coefficients converge in a nonparametric kernel regression rate instead of the usual root- n parametric rate; for time-varying coefficient models, their estimator converges in a bivariate nonparametric smoothing rate, which is much slower than classic convergence rate of varying coefficient models in Cai et al. (2000) and sensitive to bandwidth selection, as shown in our simulation studies. Also, to our knowledge, none of the existing methods adequately address the measurement error issue arising from the asynchronous variables.

To address these limitations, we propose to model the longitudinal trajectories of the covariates in the SWAN study as sparse functional data (Ramsay and Silverman, 2005), and use the functional principal component analysis (FPCA) technique (Yao et al., 2005; Li and Hsing, 2010; Zhang et al., 2016) to impute the missing synchronized covariate values from the observed asynchronous, error-prone covariate values. We then use the imputed values in second stage regression analyses. This method is similar in spirit to the regression calibration method in the measurement error literature (Carroll et al., 2006), but is completely

FUNCTIONAL CALIBRATION

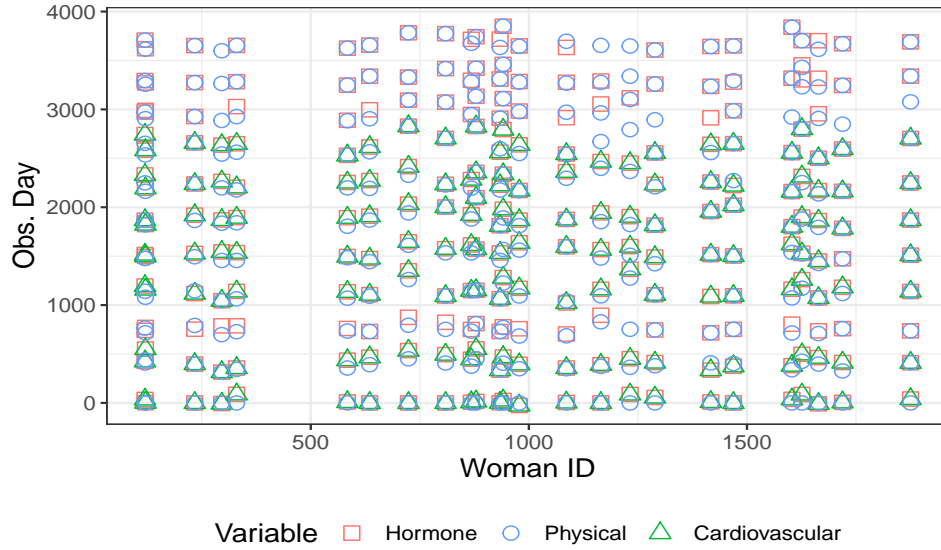


Figure 1: Observation days for a randomly selected subset of SWAN participants. Each column corresponds to one woman, with points in different colors and shapes representing variables types: hormone, physical and cardiovascular measures.

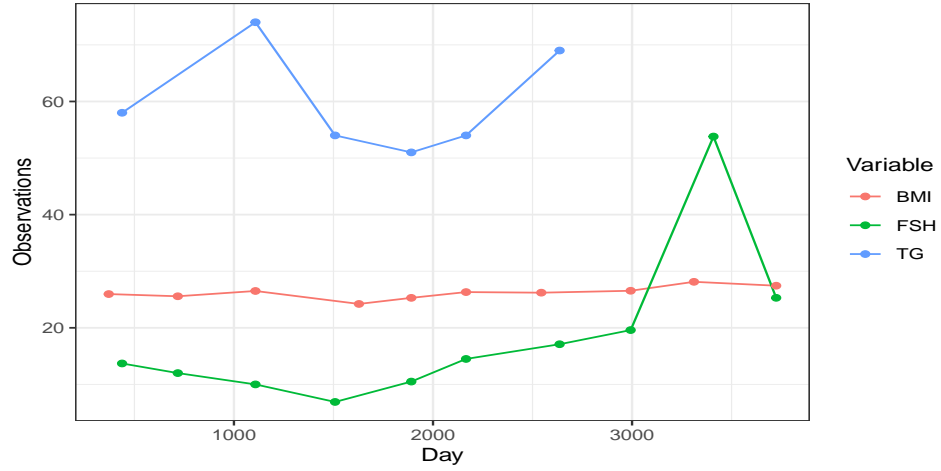


Figure 2: Longitudinal trajectories of follicle-stimulating hormone (FSH), body mass index (BMI), and triglycerides (TG) from a randomly selected SWAN participant (ID = 13959).

nonparametric. We therefore term our proposed methodology Functional Calibration for Asynchronous Regression (FCAR). The proposed method can be easily implemented using existing software, such as the ‘fdapace’ package in R, and combined with other existing re-

gression methodology such as the common linear regression with time-invariant regression coefficients and the time-varying coefficients (Hoover et al., 1998). We show that our estimators for time-invariant coefficient regression models are root- n consistent and asymptotic normal, while our estimators for time-varying coefficient models enjoy the optimal convergent rate as Hoover et al. (1998); Cai et al. (2000), which is one order of magnitude faster than the existing methods such as Cao et al. (2015). We also show that our method can be extended to accommodate multiple asynchronous longitudinal covariate processes using multivariate FPCA (Chiou et al., 2014; Happ and Greven, 2018; Dai et al., 2021).

We are aware of the related work on asynchronous longitudinal regression using functional data analysis approaches. For example, Şentürk and Müller (2010) and Şentürk et al. (2013) proposed to estimate the time-varying coefficient function by estimating the covariance function of the time-varying covariate and cross-covariance function between the covariate and response processes using bivariate kernel smoothing. However, their method is associated with the same slower bivariate smoothing convergence rate as Cao et al. (2015). Our simulation study shows our method outperforms Şentürk et al. (2013) and Cao et al. (2015) in efficiency and numerical stability. Although Şentürk et al. (2013) also considered a functional calibration method using FPCA in their numerical studies and utilized a local maximum likelihood to estimate the varying coefficient functions, their method may not be directly used to accommodate multiple time-varying covariates and no theoretical justifications were available.

The paper is organized as follows. We introduce our model assumptions in Section 2, propose the new functional calibration method and apply it to longitudinal regression models with time-invariant or time-varying coefficients in Section 3. The asymptotic properties of the proposed estimators are established in Section 4, while the practical performance of the proposed methods is illustrated by simulation studies in Section 5. In Section 6, we apply the proposed methods to analyze the SWAN data and investigate the potential effects of BMI and triglycerides on follicle-stimulating hormone changes during menopausal transition. We provide concluding remarks in Section 7, and extend the proposed method to multivariate time-varying covariate processes in Appendix B. Technical proofs and additional numerical results (tables and graphs) are respectively presented in Appendices A and C.

2. Model Assumptions

Let $\{X_i(t), Y_i(t)\}$, $i = 1, \dots, n$, be independent and identically distributed (iid) bivariate longitudinal processes defined on a compact time interval $\mathcal{T} \subset \mathbb{R}$, where $Y_i(t)$ is the response of the i th subject at time t and $X_i(t)$ is the time-varying covariate process. For simplicity, we focus on the case where $X_i(t)$ is a univariate process, and present its multivariate extension in Appendix B.

Following Cao et al. (2015), we will consider both the time-invariant coefficient model

$$Y_i(t) = \beta_0 + \beta_1 X_i(t) + \epsilon_i(t), \quad (1)$$

and the time-varying coefficient model

$$Y_i(t) = \beta_0(t) + \beta_1(t) X_i(t) + \epsilon_i(t). \quad (2)$$

In Model (1), $\boldsymbol{\beta} = (\beta_0, \beta_1)^\top$ are the time-invariant intercept and slope parameters, while $\beta_0(\cdot)$ and $\beta_1(\cdot)$ are the time-varying counterparts in Model (2). In both models, we assume $\epsilon_i(t)$ are iid zero-mean error processes with covariance function $\Omega(s, t) = \text{Cov}\{\epsilon(s), \epsilon(t)\}$. We also assume that $X_i(t)$ and $\epsilon_i(t)$ are independent of each other.

In practice, longitudinal variables are observed on discrete time points. Denote by $\mathbf{T}_i = (T_{i1}, \dots, T_{im_{y,i}})^\top$ the time points when $Y_i(\cdot)$ is observed, and by $\mathbf{Y}_i = (Y_{i1}, \dots, Y_{im_{y,i}})^\top$ the observed response vector, where $Y_{ij} = Y_i(T_{ij})$, $j = 1, \dots, m_{y,i}$. On the other hand, in an asynchronous longitudinal design, $X(t)$ are observed on time points $\mathbf{S}_i = (S_{i1}, \dots, S_{im_{x,i}})^\top$. Let $\mathbf{X}_i = (X_{i1}, \dots, X_{im_{x,i}})^\top$ where $X_{ij} = X_i(S_{ij})$, $j = 1, \dots, m_{x,i}$. As illustrated in our motivating example, \mathbf{S}_i and $m_{x,i}$ can be completely different from \mathbf{T}_i and $m_{y,i}$. In addition, these time-varying covariates are usually contaminated with measurement error. These measurement errors are not necessarily instrument error, but due to local variations. In the SWAN study, as the weight (hence BMI) and triglycerides level naturally fluctuate over days or even within the same day, it is reasonable to use their long-term or average values as the “true” values to predict the response; failing to take into account the measurement error can result in biased estimates and reduced statistical power (Carroll et al., 2006). To proceed, we relate X_{ij} , the “truth”, to its observed error-contaminated surrogates, denoted by W_{ij} , via an additive measurement error model (Carroll et al., 2006):

$$W_{ij} = X_{ij} + U_{ij}, \quad j = 1, \dots, m_{x,i}, \quad i = 1, \dots, n, \quad (3)$$

where U_{ij} are iid zero-mean measurement errors with variance σ_u^2 and independent of \mathbf{X}_i . Model (1) or (2), coupled with (3), is termed *asynchronous longitudinal regression with measurement error*.

Let $\mathbf{W}_i = (W_{i1}, \dots, W_{im_{x,i}})^\top$ be the *observed surrogate* values that are *asynchronous* with \mathbf{Y}_i , whereas we denote by $\mathbf{X}_{*i} = \{X_i(T_{i1}), \dots, X_i(T_{im_{y,i}})\}^\top$ the *unobserved true* covariate values that are *synchronized* with \mathbf{Y}_i . In the measurement error literature (Carroll et al., 2006), a commonly used technique to impute \mathbf{X}_{*i} from observed surrogate \mathbf{W}_i is regression calibration, which ignores longitudinal correlations, does not capture the dynamic changes in the time-varying covariates and may incur efficiency loss. We instead propose to calibrate the value of \mathbf{X}_{*i} using a more efficient functional data analysis approach. We assume that the time-varying covariate $X(t), t \in \mathcal{T}$ is a stochastic process defined on \mathcal{T} with mean and covariance functions

$$\mu(t) = \mathbb{E}\{X_i(t)\}, \quad R(s, t) = \text{Cov}\{X_i(s), X_i(t)\}, \quad s, t, \in \mathcal{T}.$$

The covariance function is a smooth, symmetric, positive semi-definite function with spectral decomposition $R(s, t) = \sum_{k=1}^q \omega_k \psi_k(s) \psi_k(t)$, where $\omega_1 \geq \omega_2 \geq \dots \geq \omega_q > 0$ are the eigenvalues, and $\psi_k(\cdot)$ are the corresponding eigenfunctions, also known as the principal components, such that $\int_{\mathcal{T}} \psi_k(t) \psi_{k'}(t) dt = I(k = k')$. By the Karhunen–Loève theorem (Hsing and Eubank, 2015),

$$X_i(t) = \mu(t) + \sum_{k=1}^q \xi_{ik} \psi_k(t), \quad t \in \mathcal{T}, \quad (4)$$

for $i = 1, \dots, n$, where $\xi_{ik} = \int_{\mathcal{T}} \{X_i(t) - \mu(t)\} \psi_k(t) dt$ are principal component scores with mean zero and $\text{Cov}(\xi_{ik}, \xi_{ik'}) = \omega_k I(k = k')$. The number of principal components q can be infinity in theory, but it is common to assume that $X_i(t)$ has a reduced rank representation

where q is finite (Zhou et al., 2010). This is suitable for longitudinal or sparse functional data, where the number of measurements on each trajectories is small, and one cannot realistically estimate a large number of principal components. In practice, q is chosen in a data-driven fashion (Yao et al., 2005; Li et al., 2013), which is to be detailed in Section 3.1.

3. Functional Calibration for Asynchronous Regression

3.1 Calibration using Functional Principal Component Analysis

Let $\boldsymbol{\mu}_i = \{\mu(S_{i1}), \dots, \mu(S_{im_{x,i}})\}^T$ and $\boldsymbol{\psi}_{ik} = \{\psi_k(S_{i1}), \dots, \psi_k(S_{im_{x,i}})\}^T$, $k = 1, \dots, q$, be the mean and eigenfunctions interpolated on the observed time points, and put $\boldsymbol{\Psi}_i = [\boldsymbol{\psi}_{i1}, \dots, \boldsymbol{\psi}_{iq}]$. Under the reduced rank model (4) with a finite rank q , the within-subject covariance matrix for \mathbf{W}_i is $\boldsymbol{\Sigma}_i = \text{Cov}(\mathbf{W}_i) = \boldsymbol{\Psi}_i \boldsymbol{\Lambda} \boldsymbol{\Psi}_i^T + \sigma_u^2 I$, where $\boldsymbol{\Lambda} = \text{diag}(\omega_1, \dots, \omega_q)$. If $\boldsymbol{\mu}_i$ and $\boldsymbol{\Lambda}$ were known, a roadmap for calibrating the unobserved, synchronized covariates \mathbf{X}_{*i} would be as follows. First, the best linear unbiased predictors (BLUP) for the FPC scores would be

$$\tilde{\boldsymbol{\xi}}_i = (\tilde{\xi}_{i1}, \dots, \tilde{\xi}_{iq})^T = \boldsymbol{\Lambda} \boldsymbol{\Psi}_i^T \boldsymbol{\Sigma}_i^{-1} (\mathbf{W}_i - \boldsymbol{\mu}_i). \quad (5)$$

Second, one could predict the functional trajectory of $X_i(t)$ by

$$\tilde{X}_i(t) = \mu(t) + \sum_{k=1}^q \tilde{\xi}_{ik} \psi_k(t). \quad (6)$$

Finally, interpolating these predicted trajectories on the observation times of Y , we could predict the unobserved, synchronized covariates \mathbf{X}_{*i} by

$$\tilde{\mathbf{X}}_{*i} = \boldsymbol{\mu}_{*i} + \sum_{k=1}^q \tilde{\xi}_{ik} \boldsymbol{\psi}_{*ik} = \boldsymbol{\mu}_{*i} + \boldsymbol{\Psi}_{*i} \tilde{\boldsymbol{\xi}}_i, \quad (7)$$

where $\boldsymbol{\mu}_{*i} = \{\mu(T_{i1}), \dots, \mu(T_{im_{y,i}})\}^T$, $\boldsymbol{\Psi}_{*i} = \{\boldsymbol{\psi}_{*i1}, \dots, \boldsymbol{\psi}_{*iq}\}$ and $\boldsymbol{\psi}_{*ik} = \{\psi_k(T_{i1}), \dots, \psi_k(T_{im_{y,i}})\}^T$, $k = 1, \dots, q$.

However, as $\boldsymbol{\mu}_i$ and $\boldsymbol{\Lambda}$ are unknown, and in order to complete this calibration roadmap, we need to estimate them based on the observed data $\{\mathbf{W}_i, i = 1, \dots, n\}$. Let $K(\cdot)$ be a kernel function, and denote $K_h(u) = K(u/h)/h$ where h is the bandwidth. Following Yao et al. (2005) and Li and Hsing (2010), we use local linear smoothers to estimate mean and covariance functions. For any fixed t , we estimate $\mu(t)$ by $\hat{\mu}(t) = \hat{a}_0$ where

$$(\hat{a}_0, \hat{a}_1) = \underset{a_0, a_1}{\operatorname{argmin}} \frac{1}{n} \sum_{i=1}^n \frac{1}{m_{x,i}} \sum_{j=1}^{m_{x,i}} \{W_{ij} - a_0 - a_1(S_{ij} - t)\}^2 K_{h_\mu}(S_{ij} - t),$$

with $h_\mu > 0$ being the bandwidth. We then estimate $R(s, t)$ by $\hat{R}(s, t) = \hat{a}_0$ with

$$\begin{aligned} (\hat{a}_0, \hat{a}_1, \hat{a}_2) = & \underset{a_0, a_1, a_2}{\operatorname{argmin}} \frac{1}{n} \sum_{i=1}^n \left[\frac{1}{M_{x,i}} \sum_{j \neq l} \{L_{ij} L_{il} - a_0 - a_1(S_{ij} - s) - a_2(S_{il} - t)\}^2 \right. \\ & \left. \times K_{h_R}(S_{ij} - s) K_{h_R}(S_{il} - t) \right], \end{aligned}$$

where $L_{ij} = W_{ij} - \hat{\mu}(S_{ij})$, $M_{x,i} = m_{x,i}(m_{x,i} - 1)$, and $h_R > 0$ is the bandwidth. Similarly, we can estimate the variance function $V(t) = \text{Var}\{W(t)\} = R(t, t) + \sigma_u^2$ by $\hat{V}(t) = \hat{a}_0$ where

$$(\hat{a}_0, \hat{a}_1) = \underset{a_0, a_1}{\text{argmin}} \frac{1}{n} \sum_{i=1}^n \frac{1}{m_{x,i}} \sum_{j=1}^{m_{x,i}} \{L_{ij}^2 - a_0 - a_1(S_{ij} - t)\}^2 K_{h_V}(S_{ij} - t).$$

Then we estimate σ_u^2 by

$$\hat{\sigma}_u^2 = \frac{1}{|\mathcal{T}|} \int_{\mathcal{T}} \{\hat{V}(t, t) - \hat{R}(t, t)\} dt.$$

To estimate the functional principal components, we take a spectral decomposition of $\hat{R}(s, t)$

$$\hat{R}(s, t) = \sum_k \hat{\omega}_k \hat{\psi}_k(s) \hat{\psi}_k(t),$$

which can be solved numerically by discretizing the smoothed covariance.

Let $\hat{\boldsymbol{\mu}}_i$, $\hat{\boldsymbol{\psi}}_{ik}$, $\hat{\boldsymbol{\Psi}}_i$, $\hat{\boldsymbol{\Lambda}}$, and $\hat{\boldsymbol{\Sigma}}_i$ be the estimated counterparts of $\boldsymbol{\mu}_i$, $\boldsymbol{\psi}_{ik}$, $\boldsymbol{\Psi}_i$, $\boldsymbol{\Lambda}$, and $\boldsymbol{\Sigma}_i$ using the kernel estimators described above. We adopt the PACE method of Yao et al. (2005) to estimate the principal component score ξ_{ik} by the sample version of BLUP (5)

$$\hat{\boldsymbol{\xi}}_i = (\hat{\xi}_{i1}, \dots, \hat{\xi}_{iq})^T = \hat{\boldsymbol{\Lambda}} \hat{\boldsymbol{\Psi}}_i^T \hat{\boldsymbol{\Sigma}}_i^{-1} \{\mathbf{W}_i - \hat{\boldsymbol{\mu}}_i\}. \quad (8)$$

By the expansion (4), we can recover the covariate process by

$$\hat{X}_i(t) = \hat{\mu}(t) + \sum_{k=1}^q \hat{\xi}_{ik} \hat{\psi}_k(t), \quad t \in \mathcal{T}. \quad (9)$$

The number of components q can be selected by minimizing the Akaike information criterion (AIC). There are two commonly used versions of AIC based on either a marginal log-likelihood (Rice and Wu, 2001),

$$AIC_{\text{marg}}(q) = \sum_{i=1}^n \left\{ m_i \log(2\pi) + \log(\det \hat{\boldsymbol{\Sigma}}_{iq}) + (\mathbf{W}_i - \hat{\boldsymbol{\mu}}_i)^T \hat{\boldsymbol{\Sigma}}_{iq}^{-1} (\mathbf{W}_i - \hat{\boldsymbol{\mu}}_i) \right\} + 2q, \quad (10)$$

or conditional log-likelihood (Li et al., 2013),

$$AIC_{\text{cond}}(q) = N \log \left(N^{-1} \sum_{i=1}^n \|\hat{\sigma}_u^2 \hat{\boldsymbol{\Sigma}}_{iq}^{-1} (\mathbf{W}_i - \hat{\boldsymbol{\mu}}_i)\|_2^2 \right) + N + 2nq, \quad (11)$$

where $N = \sum_{i=1}^n m_{x,i}$, $\hat{\boldsymbol{\Sigma}}_{iq} = \hat{\boldsymbol{\Psi}}_{iq} \hat{\boldsymbol{\Lambda}}_q \hat{\boldsymbol{\Psi}}_{iq}^T + \hat{\sigma}_u^2 I$, $\hat{\boldsymbol{\Lambda}}_q = \text{diag}(\hat{\omega}_1, \dots, \hat{\omega}_q)$, $\hat{\boldsymbol{\Psi}}_{iq} = [\hat{\boldsymbol{\psi}}_{i1}, \dots, \hat{\boldsymbol{\psi}}_{iq}]$, and the subscript ‘ q ’ emphasizes the dependence on the number of FPC’s.

3.2 Asynchronous Regression using Calibrated Covariates

With $\hat{\boldsymbol{\mu}}_{*i}$, $\hat{\boldsymbol{\psi}}_{*ik}$ and $\hat{\boldsymbol{\Psi}}_{*i}$ (the kernel estimates interpolated at \mathbf{T}_i instead of \mathbf{S}_i), the empirical version of the calibrated covariate $\tilde{\mathbf{X}}_{*i}$ is $\hat{\mathbf{X}}_{*i} = \hat{\boldsymbol{\mu}}_{*i} + \hat{\boldsymbol{\Psi}}_{*i} \hat{\boldsymbol{\xi}}_i$, and the design matrices using calibrated covariates are $\mathbb{X}_i = (\mathbf{1}, \hat{\mathbf{X}}_{*i})$, $i = 1, \dots, n$. The regression coefficients in Model (1) can be estimated by

$$\hat{\boldsymbol{\beta}} := (\hat{\beta}_0, \hat{\beta}_1)^T = (\mathbb{X}^T \mathbb{X})^{-1} \mathbb{X}^T \mathbf{Y}, \quad (12)$$

where $\mathbf{Y} = (\mathbf{Y}_1^T, \dots, \mathbf{Y}_n^T)^T$ and $\mathbb{X} = (\mathbb{X}_1^T, \dots, \mathbb{X}_n^T)^T$.

For Model (2), we estimate $\boldsymbol{\beta}(t) := \{\beta_0(t), \beta_1(t)\}^T$ by using the local linear estimator of Hoover et al. (1998), with the unobserved $X_i(T_{ij})$ replaced by the calibrated value $\hat{X}_i(T_{ij})$ as defined in (9). That is, we estimate $\boldsymbol{\beta}(t)$ by $\hat{\mathbf{b}}_0$ from

$$(\hat{\mathbf{b}}_0, \hat{\mathbf{b}}_1) = \underset{\mathbf{b}_0, \mathbf{b}_1}{\operatorname{argmin}} \sum_{i=1}^n \sum_{j=1}^{m_{y,i}} \{Y_{ij} - \mathbb{X}_{ij}^T \mathbf{b}_0 - \mathbb{X}_{ij}^T \mathbf{b}_1 (T_{ij} - t)\}^2 K_h(T_{ij} - t), \quad (13)$$

where $\mathbb{X}_{ij} = \{1, \hat{X}_i(T_{ij})\}^T$ and $h > 0$ is the bandwidth.

4. Asymptotic Theory

4.1 Preliminaries

For ease of exposition, we assume in the asymptotic theory that both $X(t)$ and $Y(t)$ have been centered, such that $\mu(t) \equiv 0$ in (4), $\beta_0 = 0$ in (1) and $\beta_0(t) = 0$ in (2). We focus on estimating the slope parameter β_1 and the slope function $\beta_1(t)$ in Models (1) and (2), respectively; extensions to non-centered situations are straightforward but with more notation. For any positive constant sequences $\{a_n\}$ and $\{b_n\}$, denote by $a_n \prec b_n$ if $a_n/b_n \rightarrow 0$ as $n \rightarrow \infty$.

Recall \mathbf{X}_{*i} is the unobserved covariate vector synchronized with the response \mathbf{Y}_i , $\tilde{\mathbf{X}}_{*i} = \boldsymbol{\Psi}_{*i} \tilde{\boldsymbol{\xi}}_i$ is the best linear unbiased predictor of \mathbf{X}_{*i} as defined in (7), and $\hat{\mathbf{X}}_{*i}$ is the empirical version of $\tilde{\mathbf{X}}_{*i}$ replacing the unknown functions with their kernel estimators. Let $\boldsymbol{\epsilon}_i = \{\epsilon_i(T_{i1}), \dots, \epsilon_i(T_{im_{y,i}})\}^T$ be the vector of measurement error as defined in model (1) or (2), with the covariance matrix $\boldsymbol{\Omega}_i = \{\Omega(T_{ij}, T_{ij'})\}_{j,j'=1}^{m_{y,i}}$.

We assume that the numbers of observations $(m_{x,i}, m_{y,i})$ are random with $P(2 \leq m_{x,i}, m_{y,i} \leq M) = 1$ for a constant $M < \infty$. Given $m_{x,i}$, S_{ij} are iid copies of the random variable S with a density $f_S(\cdot)$; and given $m_{y,i}$, T_{ij} are iid copies of the random variable T with a density $f_T(\cdot)$. Both $f_T(\cdot)$ and $f_S(\cdot)$ are strictly greater than 0, with bounded derivatives on \mathcal{T} . Assume that $\{X_i(t), \epsilon_i(t), m_{x,i}, m_{y,i}, \mathbf{T}_i, \mathbf{S}_i\}$ are iid tuples across i . In addition, we assume the following conditions hold.

(C.1) The kernel function $K(\cdot)$ is a symmetric probability density function on $[-1, 1]$ with

$$\sigma_K^2 := \int_{-1}^1 u^2 K(u) du < \infty, \quad \nu_0 := \int_{-1}^1 K^2(u) du < \infty.$$

(C.2) All eigenfunctions $\psi_k(t)$, $k = 1, \dots, q$, are twice differentiable, and the second derivatives $\psi_k''(t)$ are uniformly continuous on \mathcal{T} .

(C.3) There exists a constant $C > 4$ such that $E(|U_{ij}|^C) + E\left\{\sup_{t \in \mathcal{T}} |X_i(t)|^C\right\} < \infty$.

(C.4) Assume $h_R \rightarrow 0$, $h_V \rightarrow 0$ as $n \rightarrow \infty$, $(\log n/n)^{1/3} \prec h_R \prec n^{-1/4}$ and $(\log n)n^{-3/4} \prec h_V \prec n^{-1/4}$.

Remark 1. The conditions above are common in functional data analysis. Under these conditions, Li and Hsing (2010) proved that the FPCA estimators possess the following uniform convergence properties

$$\begin{aligned} \sup_{s,t \in \mathcal{T}} |\hat{R}(s,t) - R(s,t)| &= O\{h_R^2 + \sqrt{\log n/(nh_R^2)}\} \quad a.s., \\ \hat{\sigma}_u^2 - \sigma_u^2 &= O\{h_R^2 + \sqrt{\log n/(nh_R)} + h_V^2 + \log n/(nh_V)\} \quad a.s., \\ \sup_{t \in \mathcal{T}} |\hat{\psi}_k(t) - \psi_k(t)| &= O\{h_R^2 + \sqrt{\log n/(nh_R)}\} \quad a.s., \\ \hat{\omega}_k - \omega_k &= O(\sqrt{\log n/n}) \quad a.s. \quad k = 1, \dots, q. \end{aligned}$$

Recall $\tilde{X}_i(t)$ defined in (6) is the BLUP for $X_i(t)$ and $\hat{X}_i(t)$ in (9) is its empirical counterpart. By straightforward calculations,

$$\sup_{t \in \mathcal{T}} |\hat{X}_i(t) - \tilde{X}_i(t)| = O\{h_R^2 + \sqrt{\log n/(nh_R)} + h_V^2 + \log n/(nh_V)\} \quad a.s. \quad (14)$$

It is well-known in the measurement error literature (Carroll et al., 2006), replacing $X_i(t)$ with the calibrated value $E\{X_i(t) \mid \mathbf{W}_i\}$ will result in consistent but less efficient estimators. Equation (14) shows that our functional calibration $\hat{X}_i(t)$ uniformly converges to the BLUP $\tilde{X}_i(t)$, and hence our estimators in (12) and (13) are consistent; however, the derivation of their asymptotic distributions needs much involved analysis.

4.2 Asymptotic Properties of FCAR Estimator for the Time-Invariant Regression Model

The following theorem establishes the asymptotic property of the coefficient estimator (12) under the time-invariant regression model (1).

Theorem 1 *Under the assumptions above, the estimated slope parameter for model (1) has the following asymptotic distribution*

$$\sqrt{n}(\hat{\beta}_1 - \beta_1) \xrightarrow{d} Normal\{0, (\gamma_1 + \beta_1^2 \gamma_2)/\gamma_x^2\},$$

where

$$\begin{aligned} \gamma_x &= E(\tilde{\mathbf{X}}_{*i}^T \tilde{\mathbf{X}}_{*i}) = E\left\{\text{tr}\left(\Psi_{*i} \Lambda \Psi_i^T \Sigma_i^{-1} \Psi_i \Lambda \Psi_{*i}^T\right)\right\}, \\ \gamma_1 &= E\left\{\text{tr}\left(\Psi_{*i} \Lambda \Psi_i^T \Sigma_i^{-1} \Psi_i \Lambda \Psi_{*i}^T \Omega_i\right)\right\}, \\ \gamma_2 &= \text{Var}\left[\sum_{j=1}^{m_{y,i}} \tilde{X}_i(T_{ij})\{X_i(T_{ij}) - \tilde{X}_i(T_{ij})\} + \frac{1}{M_{x,i}} \sum_{j \neq j'} u_{i,jj'}^* \mathcal{A}(S_{ij}, S_{ij'})\right], \end{aligned} \quad (15)$$

$u_{i,jj'}^* = W_{ij}W_{ij'} - R(S_{ij}, S_{ij'})$, $\mathcal{A}(s_1, s_2)$ is defined in Lemma 2, and the expectations are taken over $(\mathbf{X}_i, \epsilon_i, m_{x,i}, m_{y,i}, \mathbf{T}_i, \mathbf{S}_i)$.

Remark 2. Under the special case that the BLUP $\tilde{X}_i(t)$ is also the conditional mean $E\{X_i(t) \mid \mathbf{W}_i\}$, for example when ξ_i and \mathbf{U}_i are jointly Gaussian, $\{\tilde{X}_i(t) - X_i(t), t \in$

\mathcal{T} is uncorrelated with any function of \mathbf{W}_i . One can show, under such an circumstance, $\gamma_2 = \gamma_{21} + \gamma_{22}$, where $\gamma_{21} = \text{Var}[\sum_{j=1}^{m_{y,i}} \tilde{X}_i(T_{ij})\{X_i(T_{ij}) - \tilde{X}_i(T_{ij})\}]$ and $\gamma_{22} = \text{Var}\{M_{x,i}^{-1} \sum_{j \neq j'} u_{i,jj'}^* \mathcal{A}(S_{ij}, S_{i'j'})\}$. Under the additional Gaussian assumption on ξ_i and \mathbf{U}_i , we can also obtain $\gamma_{21} = \text{E}[\text{tr}\{\Psi_{*i} \Lambda \Psi_i^T \Sigma_i^{-1} \Psi_i \Lambda \Psi_{*i}^T \Psi_{*i} \Lambda (\mathbf{I} - \Psi_i^T \Sigma_i^{-1} \Psi_i \Lambda) \Psi_{*i}^T\}]$.

As in the classic regression calibration literature (Carroll et al., 2006), one can define $\tilde{\beta}$ to be the counterpart of $\hat{\beta}$ in (12) replacing $\hat{X}_i(t)$ with $\tilde{X}_i(t)$, as if all the functional and scalar parameters in (3) and (4) are known, then $(\gamma_1 + \beta_1^2 \gamma_{21})/\gamma_x^2$ is the asymptotic variance of $\tilde{\beta}_1$. In our problem, $\beta_1^2 \gamma_{22}/\gamma_x^2$ is the additional variation caused by the FPCA estimation errors, i.e. those caused by substituting $\mu(t)$, $\psi_k(t)$, ω_k and σ_u^2 with their functional estimators described in Section 3.1. .

While it is tempting to treat the calibrated values $\hat{\mathbf{X}}_{*i}$ as the truth and use the naive standard error for linear regression to infer β_1 , the decomposition of the asymptotic variance in Theorem 1 suggests that this approach ignores the extra variations caused by calibration of the covariate values as well as estimation errors from FPCA. As a result, the naive approach leads to an underestimated variation, a low coverage rate in confidence intervals and illegitimate inferences. We recommend estimating the standard error of $\hat{\beta}$ using bootstrap, where we resample the subjects and repeat the FPCA procedure to the bootstrap samples to properly account for these extra variations.

4.3 Asymptotic Properties of FCAR Estimator for the Time-Varying Regression Model

Again we assume both $X(t)$ and $Y(t)$ are centered so that $\beta_0(t) = 0$ and we can focus on estimating $\beta_1(t)$ in Model (2). We also make the additional assumptions.

- (C.5) The slope function $\beta_1(t)$ is twice continuously differentiable on \mathcal{T} .
- (C.6) The kernel function in fitting the time-varying regression model in (13) is Lipschitz continuous and satisfies (C.1).
- (C.7) The bandwidth h in (13) satisfies $h_R/h \rightarrow 0$, $\log(n)h^5/h_R \rightarrow 0$, $nh^7 \rightarrow 0$ and $nh \rightarrow \infty$.

Theorem 2 *Under the framework outlined in Section 4.1 and assumptions (C.1)–(C.7), the estimated slope function for model (2) has the following asymptotic distribution*

$$\sqrt{nh}\Gamma_0(t)\{\hat{\beta}_1(t) - \beta_1(t) - \frac{1}{2}\beta_1^{(2)}(t)\sigma_K^2 h^2\} \xrightarrow{d} \text{Normal}[0, \Gamma_1(t) + \beta_1^2(t)\{\Gamma_2(t) + \Gamma_3(t)\}],$$

for any $t \in \mathcal{T}$, where $\bar{m}_y = \text{E}(m_{y,i})$, $\Gamma_0(t) = \bar{m}_y f_T(t) \Gamma_x(t)$,

$$\begin{aligned} \Gamma_x(t) &= \text{Var}\{\tilde{X}_i(t)\} = \boldsymbol{\psi}^T(t) \Lambda \text{E}(\Psi_i^T \Sigma_i^{-1} \Psi_i) \Lambda \boldsymbol{\psi}(t), \\ \Gamma_1(t) &= \bar{m}_y \Gamma_x(t) \Omega(t, t) f_T(t) \nu_0, \\ \Gamma_2(t) &= \bar{m}_y \text{E}[\tilde{X}^2(t) \{X(t) - \tilde{X}(t)\}^2] \nu_0, \\ \Gamma_3(t) &= \bar{m}_y^2 f_S(t) \nu_0 \left[\text{E}(M_{x,i}^{-1}) \int \Pi(t, s_2, s_2) \mathcal{Q}^2(s_2, t) f_S(s_2) ds_2 \right. \\ &\quad \left. + \text{E}\{M_{x,i}^{-1}(m_{x,i} - 2)\} \int \Pi(t, s_2, s_3) \mathcal{Q}(s_2, t) \mathcal{Q}(s_3, t) f_S(s_2) f_S(s_3) ds_2 ds_3 \right], \end{aligned}$$

$\mathcal{Q}(s, t) = \boldsymbol{\psi}^T(t) \boldsymbol{\Lambda} \mathbf{E}(\boldsymbol{\Psi}_i^T \boldsymbol{\Sigma}_i^{-1} \boldsymbol{\Psi}_i) \boldsymbol{\psi}(s) f_T(t) / \{f_S(s) f_S(t)\}$, $\Pi(s_1, s_2, s_3) = \mathbf{E}\{X^2(s_1) X(s_2) X(s_3)\} + R(s_2, s_3) \sigma_u^2 - R(s_1, s_2) R(s_1, s_3) + I(s_2 = s_3) \{R(s_1, s_1) \sigma_u^2 + \sigma_u^4\}$, and the expectations are taken over $(m_{x,i}, m_{y,i}, \mathbf{T}_i, \mathbf{S}_i, \mathbf{X}_i, \boldsymbol{\epsilon}_i)$.

Remark 3. Theorem 2 suggests that our estimator enjoys the optimal convergence rate in varying coefficient models as established in Cai et al. (2000), which is much faster than those for the competing method of Cao et al. (2015) and Şentürk and Müller (2010). Analogous to Theorem 1, $\Gamma_0^{-2}(t) \{\Gamma_1(t) + \beta_1^2(t) \Gamma_2(t)\}$ is the asymptotic variance of $\hat{\beta}_1(t)$, obtained by using $\tilde{\mathbf{X}}_{*i}$ as the predictors in the varying coefficient model (2), and $\Gamma_0^{-2}(t) \beta_1^2(t) \Gamma_3(t)$ is the extra variation caused by the FPCA errors. We therefore recommend to make inference on $\boldsymbol{\beta}(t)$ using a bootstrap procedure that accounts for the FPCA estimation error as described in Remark 2. Also Assumptions (C.4) and (C.7) require undersmoothing in the FPCA procedure; we need $h_R/h \rightarrow 0$ so that the biases caused by FPCA estimation are asymptotically negligible compared with the smoothing bias in varying coefficient models.

5. Simulation Studies

We conduct simulations to examine the finite sample performances of the time-invariant regression model (1) and time-varying coefficient model (2), and compare them with those of various exiting methods.

5.1 Simulation 1: FCAR for time-invariant coefficient model

Let the time domain be $\mathcal{T} = [0, 10]$, $X_i(t)$ be iid copies of a stochastic process described by model (4) with $q = 3$ principal components, and $\boldsymbol{\xi}_i \sim \text{Normal}\{\mathbf{0}, \text{diag}(4, 2, 1)\}$. Set $n = 200$ and generate $Y_i(t)$ from Model (1) with $\beta_0 = 1$ and $\beta_1 = 2$. Suppose there are $m = 5$ discrete observations on $X_i(t)$ and $Y_i(t)$, respectively, where $\{S_{i1}, \dots, S_{im}\}$ and $\{T_{i1}, \dots, T_{im}\}$ are generated independently from a uniform distribution on \mathcal{T} . Error-contaminated discrete observations \mathbf{W}_i are generated from Model (3) with $U_{ij} \sim \text{Normal}(0, 1)$. We consider two settings for the mean and eigenfunctions of $X_i(t)$:

- *Setting I:* $\mu(t) = t + \sin(t)$, $\psi_k(t) = (1/\sqrt{5}) \sin(\pi k t/10)$, $t \in \mathcal{T}$, $k = 1, 2, 3$;
- *Setting II:* $\mu(t) = \sin(t)$, $\psi_1(t) = \sqrt{10}$, $\psi_2(t) = \sqrt{5} \sin(2\pi t/10)$, $\psi_3(t) = \sqrt{5} \cos(2\pi t/10)$.

We generate $\epsilon_i(t)$ from a zero-mean Gaussian process with covariance function $\Omega(s, t) = \text{Cov}\{\epsilon_i(s), \epsilon_i(t)\}$, and consider two different covariance structures: 1) independent errors with $\Omega(s, t) = 1.5I(s = t)$ and 2) dependent errors with $\Omega(s, t) = 2^{-|t-s|/5}$.

For each setting and each error correlation structure, we simulate 200 data sets and apply the proposed FCAR method to each simulated data set. Specifically, FPCA is performed using the `fdapace` package of R with its built-in bandwidth selector and q is selected by the marginal likelihood *AIC*. In Table 1, we summarize the performance of $\hat{\beta}_1$ under both settings and both error covariance structures. The criteria include the bias, standard deviation, mean of the naive standard error pretending the calibrated values are the true covariates, coverage rate of a 95% confidence interval using the naive SE, mean of the bootstrap standard error, and coverage rate of a 95% confidence interval using the bootstrap SE. The results on $\hat{\beta}_0$ are similar but less interesting and hence omitted. It appears that the bias

of our estimator is much smaller than the standard deviation, corroborating Theorem 1 that $\hat{\beta}_1$ is asymptotically unbiased. The results also support Remark 2 that the naive standard error estimator underestimates the standard error and results in confidence intervals with lower than nominal coverage rates. In contrast, bootstrap standard errors capture the extra variations caused by calibrating the covariate value and FPCA estimation errors, and as a result the confidence intervals based on bootstrap standard errors yield coverage rates close to the nominal ones. As noted in Remark 2, we perform FPCA to each bootstrap sample, and Table 1 is based on 500 bootstrap samples.

Error type	Setting I		Setting II	
	independent	dependent	independent	dependent
Bias	0.007	0.004	-0.008	-0.013
SD	0.028	0.029	0.127	0.122
Naive SE	0.019	0.017	0.064	0.058
Naive CP	0.830	0.770	0.670	0.640
Bootstrap SE	0.030	0.030	0.117	0.119
Bootstrap CP	0.955	0.950	0.925	0.930

Table 1: Simulation 1: performance of $\hat{\beta}_1$ under the proposed FCAR method under different scenarios, including bias, standard deviation, mean of the naive standard error, coverage rate of a 95% confidence interval using the naive SE, mean of the bootstrap standard error, and coverage rate of a 95% confidence interval using the bootstrap SE.

Table 2 compares the proposed FCAR method with the kernel weighted (KW) method (Cao et al., 2015) and the last-observation-carry-forward (LOCF) method in biases, Monte Carlo standard deviations, and the average estimated standard errors. For the KW method, we use the function `asynchTI` from the R package `AsynchLong` (Cao et al., 2015), which provides a built-in standard error estimator. For LOCF, we impute the unobserved covariate value at T_{ij} by its nearest observation prior to T_{ij} . The bootstrap functional data procedure is not appropriate for LOCF, because it assumes covariate stops changing after a certain point, which does not conform to a functional data context; instead, we use the naive standard error for the LOCF coefficient estimates. Under both simulation settings and both error structures, the LOCF estimator for β_1 has significant negative biases; the KW method reduces biases but still yields a bias much bigger than the standard error. As a result, the confidence intervals for both LOCF and KW have coverage rates close to 0. The proposed FCAR estimator, on the other hand, has negligible bias, and yields confidence intervals with a correct coverage rate.

5.2 Simulation 2: FCAR for time-varying coefficient model

We simulate data from the time-varying coefficients regression model (2). As in Simulation 1, we set the time domain to be $\mathcal{T} = [0, 10]$ and simulate $n = 200$ subjects with $m_i = 5$ repeated measures on $X_i(t)$ and $Y_i(t)$ allowing the measuring time points to be asynchronous between X and Y . We simulate $X(t)$ using the Karhunen-Loève expansion

		Independent error			Dependent error		
		FCAR	KW	LOCF	FCAR	KW	LOCF
Setting I	Bias	0.007	-0.225	-0.461	0.004	-0.213	-0.464
	SD	0.028	0.067	0.043	0.029	0.067	0.043
	SE	0.030	0.049	0.045	0.030	0.051	0.044
	CP	0.955	0.060	0.000	0.950	0.065	0.000
Setting II	Bias	-0.008	-0.978	-1.357	-0.013	-0.978	-1.366
	SD	0.127	0.097	0.070	0.122	0.092	0.068
	SE	0.117	0.076	0.054	0.119	0.077	0.051
	CP	0.925	0.000	0.000	0.930	0.000	0.000

Table 2: Simulation 1: comparison of $\hat{\beta}_1$ using the proposed FCAR method with those from the kernel weighted (KW) method of (Cao et al., 2015) and the last-observation-carry-forward (LOCF) method on bias, standard deviation, mean of standard error and coverage rate of a 95% confidence interval using standard error.

(4), with mean function $\mu(t) = t + \sin(t)$, $q = 3$, $\xi_i \sim \text{Normal}\{\mathbf{0}, \text{diag}(4, 2, 1)\}$ and $\psi_k(t) = (1/\sqrt{5})\sin(\pi kt/10)$, $k = 1, 2, 3$. We simulate discrete observations W_{ij} from (3) where U_{ij} are iid standard normal, and simulate Y_{ij} from (2), where the measurement error $\epsilon_i(t)$ is generated from a mean zero Gaussian process with covariance $\text{Cov}\{\epsilon_i(s), \epsilon_i(t)\} = 2^{-|t-s|/5}$. For each subject, the observation time points $\{S_{ij}\}$ and $\{T_{ij}\}$ are uniformly distributed on \mathcal{T} and independent from each other. We consider the following two settings for the time-varying coefficients

- *Setting I*: $\beta_0(t) = 0.2t + 0.5$, $\beta_1(t) = \sin(\pi t/10)$,
- *Setting II*: $\beta_0(t) = t^{1/2}$, $\beta_1(t) = \sin(\pi t/5)$.

We perform functional calibration using the **fdapace** package with *AIC* as the principal component selection criterion. To fit a time-varying coefficients model after the functional calibration, we used the **tvLM** function in the R package **tvReg** which implements the kernel smoothing method in Hoover et al. (1998) and its built-in cross-validation procedure to choose the bandwidth. For comparison, we also implement the Oracle estimator where synchronized true value of X are known, LOCF, KW of (Cao et al., 2015), and the functional varying coefficients model (FVCM) of Şentürk et al. (2013). Both the Oracle and LOCF estimators are calculated using the **tvReg** package, where LOCF simply uses the nearest last observation as surrogate of the true X value. The KW method for time-varying coefficient model is implemented using the authors’s own **asynchTD** function in the **AsynchLong** package. The FVCM method requires estimation of the covariance function of $X(t)$ and the cross-covariance function between $X(\cdot)$ and $Y(\cdot)$, which are calculated using the **fdapace** package. Bandwidths for all methods are selected using the built-in options of the packages mentioned above: generalized cross-validation of **fdapace**, cross-validation of **tvReg** and adaptive selection procedure of **AsynchLong**.

We repeat the simulation 200 times for both settings and apply the proposed and competing methods to each data set. Following Şentürk and Müller (2010), we compare different

methods using two evaluation criteria: the mean absolute deviation error (MADE) and the weighted average squared error (WASE)

$$\text{MADE} = \frac{1}{2|\mathcal{T}|} \sum_{r=0}^1 \frac{\int_{\mathcal{T}} |\hat{\beta}_r(t) - \beta_r(t)| dt}{\text{range}(\beta_r)}, \quad \text{WASE} = \frac{1}{2|\mathcal{T}|} \sum_{r=0}^1 \frac{\int_{\mathcal{T}} \{\hat{\beta}_r(t) - \beta_r(t)\}^2 dt}{\text{range}^2(\beta_r)},$$

where $\text{range}(\beta_r)$ is the range of function $\beta_r(t)$, $r = 0, 1$.

	Method	Criterion	Mean(SD)	Median	25%	75%
Setting I	FCAR	MADE	0.319(0.151)	0.302	0.207	0.388
	FVCM		1.494(2.521)	0.948	0.756	1.418
	KW		1.452(3.533)	1.026	0.868	1.297
	LOCF		0.912(0.048)	0.915	0.875	0.943
	Oracle		0.209(0.091)	0.192	0.142	0.269
	FCAR	WASE	0.345(0.395)	0.224	0.103	0.402
	FVCM		461.495(5235.731)	3.433	1.576	9.553
	KW		1057.299(14234.414)	3.830	1.716	15.221
	LOCF		1.356(0.137)	1.351	1.269	1.450
	Oracle		0.216(0.242)	0.111	0.058	0.294
Setting II	FCAR	MADE	0.263(0.104)	0.246	0.186	0.321
	FVCM		0.944(1.551)	0.616	0.440	0.913
	KW		1.153(1.669)	0.720	0.605	1.115
	LOCF		0.585(0.025)	0.585	0.570	0.602
	Oracle		0.180(0.062)	0.172	0.137	0.220
	FCAR	WASE	0.316(0.351)	0.200	0.093	0.394
	FVCM		299.501(3746.442)	1.464	0.613	5.921
	KW		204.128(1538.798)	2.709	1.196	15.833
	LOCF		0.721(0.058)	0.718	0.685	0.756
	Oracle		0.287(0.347)	0.183	0.088	0.330

Table 3: Simulation 2: MADE and WASE of various methods: mean (standard deviation), median, 25% quantile, 75% quantile.

As summarized in Table 3, the proposed FCAR method yields MADE and WASE that are much lower than LOCF and close to the Oracle estimator. The FVCM and KW methods equipped with built-in tuning parameter selectors perform worse than LOCF, likely because both of them, by evoking bivariate kernel smoothing while estimating univariate coefficient functions in Model (2), are numerically unstable.

MADE and WASE are overall numerical summaries combining $\hat{\beta}_0(\cdot)$ and $\hat{\beta}_1(\cdot)$; we also provide graphical summaries of $\hat{\beta}_0(\cdot)$ and $\hat{\beta}_1(\cdot)$ separately. In Figures 3 and 4, we summarize $\hat{\beta}_1(t)$ by all 5 methods mentioned above and for the two simulation settings respectively. As seen, the LOCF estimator for $\beta_1(t)$ is significantly biased toward 0, due to the well-known attenuation effect in the measurement error literature (Carroll et al., 2006). The proposed FCAR estimator for $\beta_1(t)$ has negligible biases compared with LOCF and overall performance comparable to the Oracle estimator. In contrast, with slower convergence rates

and numerical instability of bivariate kernel smoothing, the KW and FVCM estimators for $\beta_1(t)$ are highly variable and affected by the boundary effect. Graphical summaries of $\hat{\beta}_0(t)$ allude to the same message. We therefore relegate the graphs on $\hat{\beta}_0(t)$ under these two settings to Figures C.1 and C.2 in Appendix C.

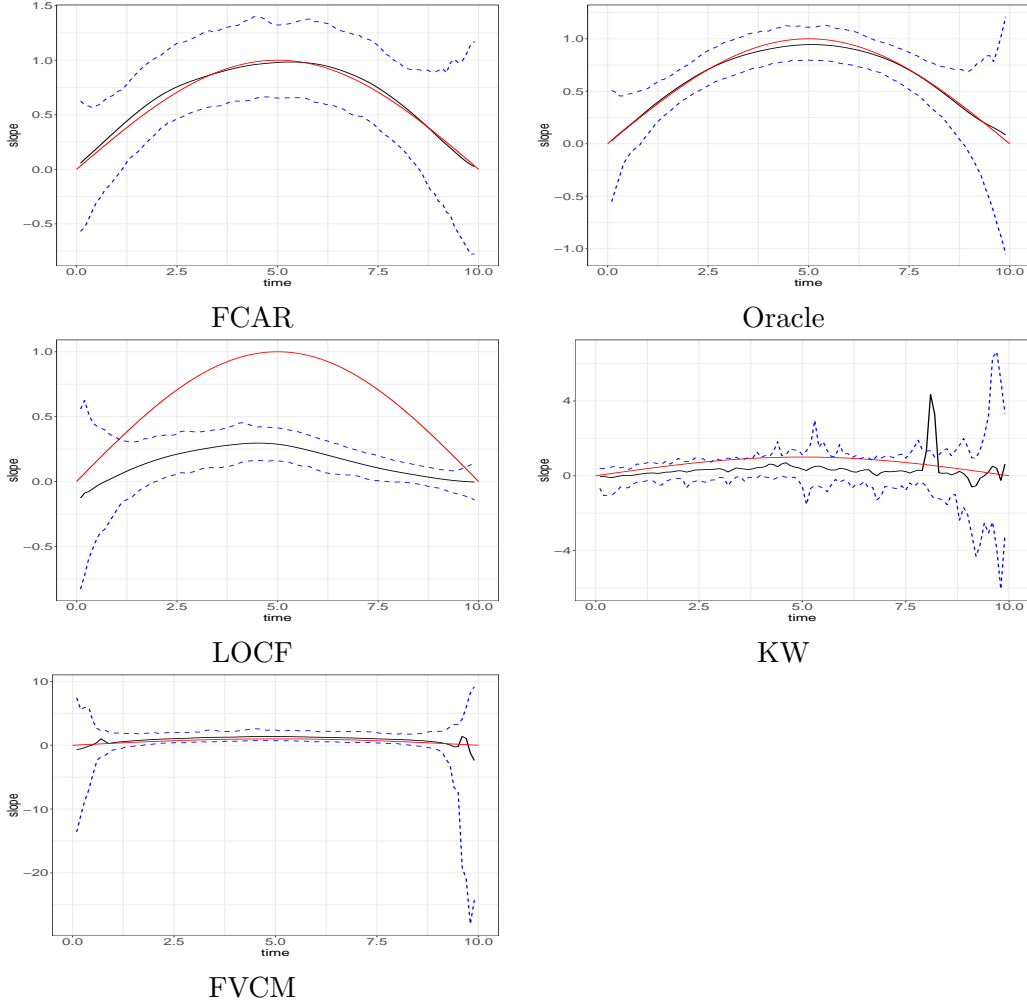


Figure 3: Summary of $\hat{\beta}_1(t)$ under Simulation 2, Setting I using various methods. In each panel, black: average of $\hat{\beta}_1(t)$, red: true $\beta_1(t)$, dashed blue: 0.975 and 0.025 quantiles.

6. Real Data Analysis

We apply the proposed FCAR method to the SWAN data described in Section 1. SWAN (Bromberger et al., 2010) was a large longitudinal observational study on women's health during menopausal transition, which plays an essential role in elderly women's lives and is associated with changes in hormone levels, cardiovascular risk factors and other physi-

FUNCTIONAL CALIBRATION

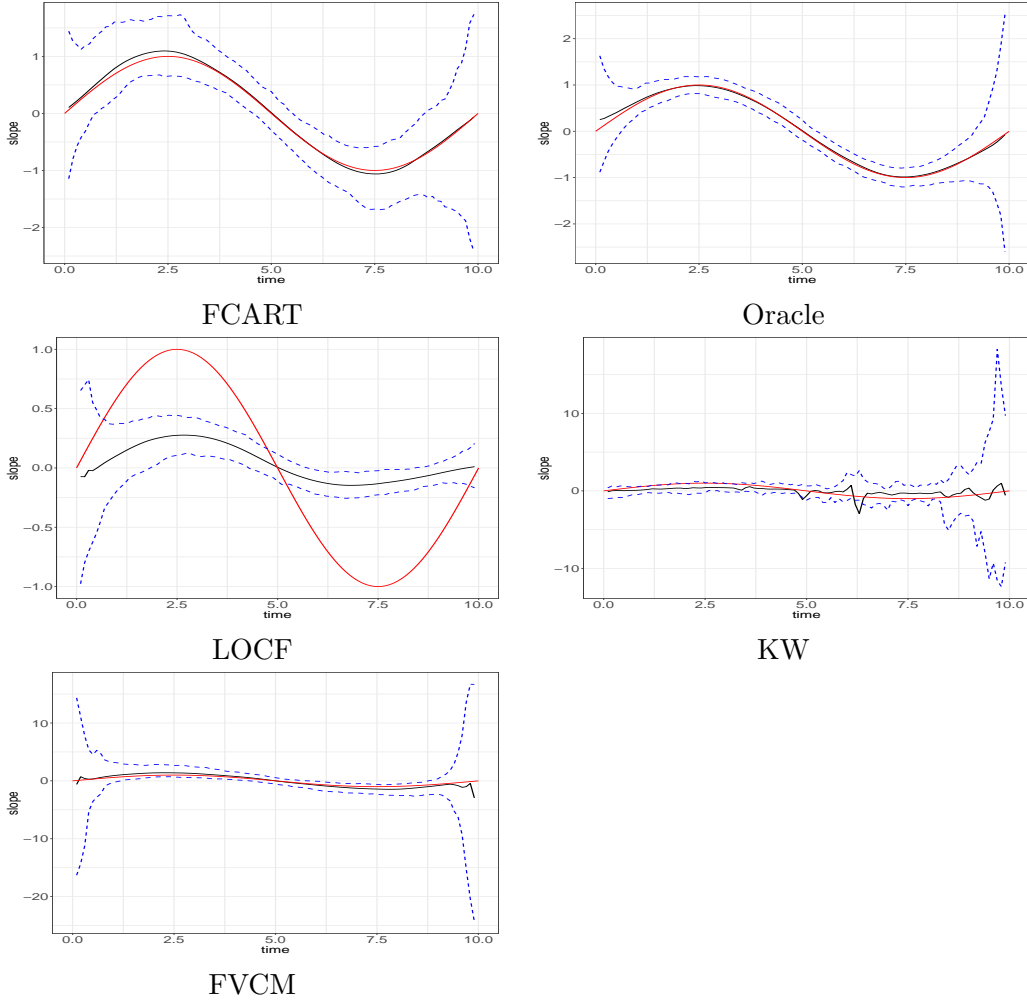


Figure 4: Summary of $\hat{\beta}_1(t)$ under Simulation 2, Setting II using various methods. In each panel, black: average of $\hat{\beta}_1(t)$, red: true $\beta_1(t)$, dashed blue: 0.975 and 0.025 quantiles.

cal measures. The study admitted 3,302 premenopausal or early perimenopausal women between 1996 and 1997, with the baseline age ranging from 42 to 53. These women were scheduled to have annual followups up to 10 years, although various hormonal, physical and cardiovascular biomarkers were measured according different schedules as illustrated in Figures 1 and 2 until the study ended in 2008.

One of the most important biomarkers in menopausal studies is the follicle-stimulating hormone (FSH) level, the outcome variable of our primary interest. As declining follicular reserve is the immediate cause of the perimenopausal and menopausal transitions (Richardson et al., 1987), an increase in the serum FSH level was one of the major endocrine changes associated with menopausal transitions (Burger et al., 1995). FSH levels rise progressively before the final menses and will continue for 2–4 years, before remaining elevated

postmenopause (Burger et al., 1999). Changes in FSH levels have been linked to or are precursors of various medical conditions. For example, abnormal variations of FSH levels are related to the depressive symptoms during the menopausal transition (Bromberger et al., 2010), and may also increase women’s risk of developing cardiovascular disease after menopause (El Khoudary et al., 2016).

Therefore, studying the dynamic relationship between FSH and other physiological measurements is of great importance to understand women’s reproductive life and their midlife health (Bromberger et al., 2010). Following Wang et al. (2020), we study the association between FSH and triglycerides (TG) adjusting for age, income level and body mass index (BMI). FSH was measured every year for the SWAN participants following the hormone measurement schedule in Figure 1, whereas TG and BMI were following the cardiovascular and physical measurement schedules in Figure 1. Of note, TG was not collected in year 2 or beyond year 8, and 47.5% of BMI measurements were asynchronous with FSH. We also included the baseline age and income as time-invariant covariates, where the income was dichotomized (1 if annual income is more than \$50k and 0 otherwise). After removing subjects with missing incomes, there are 1,634 high income subjects and 1,578 low income subjects in the data. We focus our analysis on the first 8 years of the study, when FSH, TG and BMI are all available. An added rationale behind this truncation is that all participants experienced the entire menopausal transition by year 8, becoming postmenopausal or late perimenopausal afterwards (Bromberger et al., 2010).

Existing works, such as Wang et al. (2020), assume the association between FSH and the covariates are time-invariant and ignore asynchronous issue in this data set, which may mask some intriguing time-varying associations. Instead, we apply the time-varying coefficients model to model the dynamic relationship between FSH and other time varying or invariant covariates. Among the competing methods described in Section 5.2, the kernel weighted estimator (KW) requires that all time-varying covariates are measured at the same time points, which is not applicable in our data since TG and BMI are measured on different time as well; the functional varying coefficient model (FVCM) of Şentürk and Müller (2010) was proposed for univariate time-varying covariates and is not readily applicable to multiple time-varying covariates in this data set. We therefore apply the LOCF method and our proposed FCAR method to the data.

To accommodate two time-varying covariates in our data, we slightly extend the proposed FPCA to a multivariate setting as described in Appendix B and implement it by using the `fdapace` package in R, where a built-in generalized cross-validation (GCV) procedure is used to select the bandwidths for mean and cross-covariance estimations. We then use the conditional AIC described in (11) by Li et al. (2013) to select the number of principal components for TG and BMI separately. To implement the undersmoothing scheme described in condition (C.7), we multiply the GCV selected bandwidths by a factor of $n^{-1/10}$, refit FPCA using the undersmoothing bandwidths, and then use the FPCA calibrated values for further analysis.

Both the LOCF and FCAR methods use the local polynomial method of (Hoover et al., 1998) to estimate the time-varying coefficients in Model (B.2). To make the results comparable, we use the same bandwidth to fit Model (B.2). Fig 5 shows the estimated coefficient functions for the two time-varying covariates, TG and BMI, using FCAR and LOCF, respectively, where 95% pointwise confidence intervals are obtained using bootstrap. As

commented in Remarks 2 and 3, we resample the subjects, perform FPCA using the same bandwidth as in real data to every bootstrap sample in order to properly take into account the FPCA estimation errors. The pointwise confidence intervals in Fig 5 are based on a normal approximation suggested by Theorem 2, where the pointwise standard error is estimated based on 200 bootstrap replicates.

As shown in Fig 5c and 5d, LOCF and FCAR provide similar results for the coefficient function BMI. These results show that FSH is negatively associated with BMI and the relationship becomes stronger through the menopausal transition. However, the two methods provide very different results for TG in Fig 5a and 5b. The estimated coefficient function by LOCF method is significantly attenuated toward 0, as we have observed in our simulation studies. The pointwise confidence intervals for the LOCF estimator mostly cover 0, suggesting a non-significant effect of TG. The FCAR estimator, on the other hand, reveals a significant negative association between TG and FSH, which grows stronger as women age. Our FCAR results are consistent with Wang et al. (2020) and Wang et al. (2017), which also detected significant negative associations of both BMI and TG with FSH among the perimenopausal and postmenopausal women.

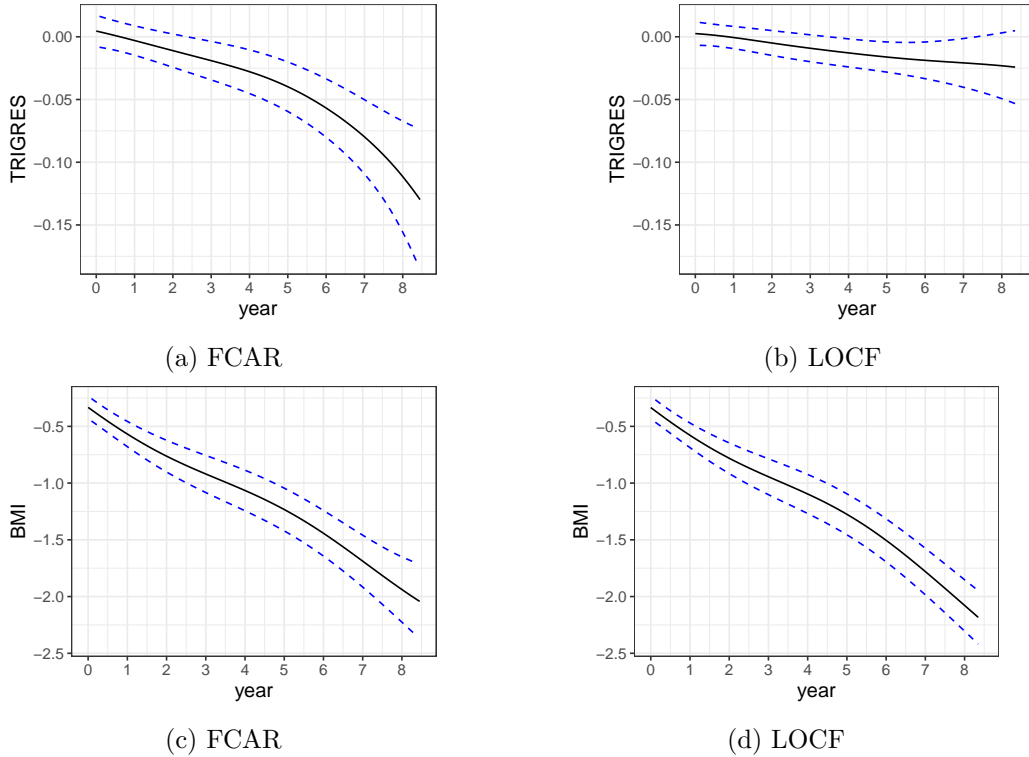


Figure 5: SWAN data analysis: time-varying coefficient model on FSH against TG, BMI, age and income. Top row: coefficient function for TG; bottom row: coefficient function for BMI. Left column: FCAR; right column: LOCF. In each panel, the solid curve is the estimated coefficient function and the dashed curves are 95% point-wise confidence intervals obtained using bootstrap.

The estimated coefficient functions for age and income are relegated to Figures C.3 and C.4 in Appendix B, because these covariates are time-invariant and their estimated coefficient functions based on FCAR and LOCF have no visible differences. These variables are confounders, whose effects are less interesting but need to be adjusted for in our analysis. We see a positive association between age and FSH, consistent with the literature that FSH is elevated during menopause transition. Interestingly, high income is negatively associated with FSH.

7. Conclusions

We have proposed a new functional calibration method, termed Functional Calibration for Asynchronous Regression (FCAR), for learning sparse asynchronous longitudinal data. The key idea behind the approach is to calibrate the missing synchronized covariates by the functional principal component analysis (FPCA) approach, which can be easily implemented using existing software. More broadly, our method is applicable to asynchronous longitudinal regression with time-invariant or time-varying coefficients, and addresses a serious limitation of the existing literature that the naive LOCF method leads to biased estimator of the coefficients, which are attenuated toward 0. Indeed, our FCAR estimator in a time-invariant regression model enjoys nice asymptotic properties, such as root- n consistency and asymptotic normality; our estimator for a time-varying coefficient model enjoys the same optimal convergence rate as those in the literature, such as Cai et al. (2000). By implementing an undersmoothing scheme in our functional calibration method, the FPCA estimation errors cause a negligible bias to the estimated model, but will inflate the asymptotic variance of the final estimator. Based on these theoretical findings, we recommend to use bootstrap standard error that takes into account FPCA errors, rather than using naive standard errors. Our theoretical analysis as well as our empirical studies show that our proposed method outperforms the existing methods, including the kernel weighted estimator of Cao et al. (2015) and the FVCM method of Şentürk and Müller (2010).

As demonstrated in Appendix B and our real data analysis, the proposed FCAR method can be easily implemented for multiple asynchronous time-varying covariates, when the number of time-varying covariates is not too high. When this number is high, the computation burden of multivariate FPCA (mFPCA) can quickly grow out of control as we will have too many cross-covariance functions to estimate, and the mFPCA estimators may become unstable. In this setting, selecting the relevant time-varying covariates becomes a challenging ‘model selection with error-in-variable’ problem, because the calibrated covariate values contain estimation errors that are not independent and have complicated structures. These challenges warrant future investigations.

Acknowledgements

The work is partially supported by grants from the National Institutes of Health. The data and code are available at https://github.com/chxyself25/Functional_Calibration.

References

- Joyce T Bromberger, Laura L Schott, Howard M Kravitz, MaryFran Sowers, Nancy E Avis, Ellen B Gold, John F Randolph, and Karen A Matthews. Longitudinal change in reproductive hormones and depressive symptoms across the menopausal transition: results from the study of women's health across the nation (swan). *Archives of general psychiatry*, 67(6):598–607, 2010.
- Henry G Burger, Emma C Dudley, John L Hopper, Julia M Shelley, Adele Green, Anthony Smith, Lorraine Dennerstein, and Carol Morse. The endocrinology of the menopausal transition: a cross-sectional study of a population-based sample. *The Journal of Clinical Endocrinology & Metabolism*, 80(12):3537–3545, 1995.
- Henry G Burger, Emma C Dudley, John L Hopper, Nigel Groome, Janet R Guthrie, Adele Green, and Lorraine Dennerstein. Prospectively measured levels of serum follicle-stimulating hormone, estradiol, and the dimeric inhibins during the menopausal transition in a population-based cohort of women. *The Journal of Clinical Endocrinology & Metabolism*, 84(11):4025–4030, 1999.
- Zongwu Cai, Jianqing Fan, and Runze Li. Efficient estimation and inferences for varying-coefficient models. *Journal of the American Statistical Association*, 95(451):888–902, 2000.
- Hongyuan Cao, Donglin Zeng, and Jason P Fine. Regression analysis of sparse asynchronous longitudinal data. *Journal of the Royal Statistical Society, Series B*, 77:755–776, 2015.
- Hongyuan Cao, Jialiang Li, and Jason P Fine. On last observation carried forward and asynchronous longitudinal regression analysis. *Electronic Journal of Statistics*, 10:1155 – 1180, 2016.
- Raymond J Carroll, David Ruppert, Leonard A Stefanski, and Ciprian M Crainiceanu. *Measurement Error in Nonlinear Models: A Modern Perspective*. Chapman and Hall/CRC, Boca Raton, FL, 2006.
- Jeng-Min Chiou, Yu-Ting Chen, and Ya-Fang Yang. Multivariate functional principal component analysis: a normalization approach. *Statistica Sinica*, 24:1571–1596, 2014.
- Richard J Cook, Leilei Zeng, and Grace Y Yi. Marginal analysis of incomplete longitudinal binary data: a cautionary note on locf imputation. *Biometrics*, 60:820–838, 2004.
- Xiongtao Dai, Zhenhua Lin, and Hans-Georg Müller. Modeling sparse longitudinal data on riemannian manifolds. *Biometrics*, 77(4):1328–1341, 2021.
- Samar R El Khoudary, Nanette Santoro, Hsiang-Yu Chen, Ping G Tepper, Maria M Brooks, Rebecca C Thurston, Imke Janssen, Sioban D Harlow, Emma Barinas-Mitchell, Faith Selzer, et al. Trajectories of estradiol and follicle-stimulating hormone over the menopause transition and early markers of atherosclerosis after menopause. *European Journal of Preventive Cardiology*, 23(7):694–703, 2016.

- Clara Happ and Sonja Greven. Multivariate functional principal component analysis for data observed on different (dimensional) domains. *Journal of the American Statistical Association*, 113(522):649–659, 2018.
- Donald R Hoover, John A Rice, Colin O Wu, and Li-Ping Yang. Nonparametric smoothing estimates of time-varying coefficient models with longitudinal data. *Biometrika*, 85(4):809–822, 1998.
- Tailen Hsing and Randall Eubank. *Theoretical Foundations of Functional Data Analysis, with an Introduction to Linear Operators*. Wiley, Chichester, UK, 2015.
- Yehua Li and Tailen Hsing. Uniform convergence rates for nonparametric regression and principal component analysis in functional/longitudinal data. *Annals of Statistics*, 38:3321–3351, 2010.
- Yehua Li, Naisyin Wang, and Raymond J Carroll. Selecting the number of principal components in functional data. *Journal of the American Statistical Association*, 108(504):1284–1294, 2013.
- Geert Molenberghs, Herbert Thijs, Ivy Jansen, Caroline Beunckens, Michael G Kenward, Craig Mallinckrodt, and Raymond J Carroll. Analyzing incomplete longitudinal clinical trial data. *Biostatistics*, 5:445–464, 2004.
- James O Ramsay and Bernhard W Silverman. *Functional Data Analysis*. Springer-Verlag,, New York, 2nd edition, 2005.
- John A Rice and Colin O Wu. Nonparametric mixed effects models for unequally sampled noisy curves. *Biometrics*, 57(1):253–259, 2001.
- Sandra J Richardson, Vyta Senikas, and James F Nelson. Follicular depletion during the menopausal transition: evidence for accelerated loss and ultimate exhaustion. *The Journal of Clinical Endocrinology & Metabolism*, 65(6):1231–1237, 1987.
- James M Robins, Andrea Rotnitzky, and Lue Ping Zhao. Analysis of semiparametric regression models for repeated outcomes in the presence of missing data. *Journal of American Statistical Association*, 90:106–121, 1995.
- Damla Şentürk and Hans-Georg Müller. Functional varying coefficient models for longitudinal data. *Journal of the American Statistical Association*, 105(491):1256–1264, 2010.
- Damla Şentürk, Lorien S Dalrymple, Sandra M Mohammed, George A Kaysen, and Danh V Nguyen. Modeling time-varying effects with generalized and unsynchronized longitudinal data. *Statistics in Medicine*, 32(17):2971–2987, 2013.
- Ningjian Wang, Hongfang Shao, Yi Chen, Fangzhen Xia, Chen Chi, Qin Li, Bing Han, Yincheng Teng, and Yingli Lu. Follicle-stimulating hormone, its association with cardiometabolic risk factors, and 10-year risk of cardiovascular disease in postmenopausal women. *Journal of the American Heart Association*, 6(9):e005918, 2017.

Xue Wang, Hongyan Zhang, Yijie Chen, Yini Du, Xuejing Jin, and Zhifen Zhang. Follicle stimulating hormone, its association with glucose and lipid metabolism during the menopausal transition. *Journal of Obstetrics and Gynaecology Research*, 46(8):1419–1424, 2020.

Fang Yao, Hans-Georg Müller, and Jane-Ling Wang. Functional data analysis for sparse longitudinal data. *Journal of the American Statistical Association*, 100(470):577–590, 2005.

Xiaoke Zhang, Jane-Ling Wang, et al. From sparse to dense functional data and beyond. *The Annals of Statistics*, 44(5):2281–2321, 2016.

Lan Zhou, Jianhua Z Huang, Josue G Martinez, Arnab Maity, Veerabhadran Baladandayuthapani, and Raymond J Carroll. Reduced rank mixed effects models for spatially correlated hierarchical functional data. *Journal of the American Statistical Association*, 105:390–400, 2010.

Appendix A: Technical Proofs

A.1 Preliminaries

Recall that we use the subscript $*$ to denote the covariates and eigenfunctions evaluated on the same time points as the response, and $\mathbf{X}_{*i} = \{X_i(T_{i1}), \dots, X_i(T_{im_{y,i}})\}^T$, $\Psi_i = (\psi_{i1}, \dots, \psi_{iq})$ and $\Psi_{*i} = (\psi_{*i1}, \dots, \psi_{*iq})$, where $\psi_{ik} = \{\psi_k(S_{i1}), \dots, \psi_k(S_{im_{x,i}})\}^T$ and $\psi_{*ik} = \{\psi_k(T_{i1}), \dots, \psi_k(T_{im_{y,i}})\}^T$.

Put $\mathbf{X}_* = (\mathbf{X}_{*1}^T, \dots, \mathbf{X}_{*n}^T)^T$, $\mathbf{\Lambda} = \text{diag}(\omega_1, \dots, \omega_K)$, and the FPCA score vectors as $\xi_i = (\xi_{i1}, \dots, \xi_{iq})^T$. and the observed covariance matrix is $\Sigma_i = \Psi_i \mathbf{\Lambda} \Psi_i^T + \sigma_u^2 \mathbf{I}$. Specifically, the conditional mean and estimator for \mathbf{X}_{*i} are

$$\tilde{\mathbf{X}}_{*i} = \Psi_{*i} \tilde{\xi}_i = \Psi_{*i} \mathbf{\Lambda} \Psi_i^T (\Psi_i \mathbf{\Lambda} \Psi_i^T + \sigma_u^2 \mathbf{I})^{-1} \mathbf{W}_i \quad (\text{A.1})$$

$$\hat{\mathbf{X}}_{*i} = \hat{\Psi}_{*i} \hat{\xi}_i = \hat{\Psi}_{*i} \hat{\mathbf{\Lambda}} \hat{\Psi}_i^T (\hat{\Psi}_i \hat{\mathbf{\Lambda}} \hat{\Psi}_i^T + \hat{\sigma}_u^2 \mathbf{I})^{-1} \mathbf{W}_i. \quad (\text{A.2})$$

Define $\delta_{n1}(h) = \{h^{-1} \log n/n\}^{1/2}$, $\delta_{n2}(h) = \{h^{-2} \log n/n\}^{1/2}$, and $\zeta_n(h) = \sqrt{nh^2} + h^{1/2} + h^{-1/2} \delta_{n2}(h)$.

Lemma 1 *Under assumptions described in Section 4.1, for $t \in \mathcal{T}$,*

$$\begin{aligned} \hat{\psi}_k(t) - \psi_k(t) &= \frac{1}{n} \sum_{i=1}^n \frac{1}{M_{x,i}} \sum_{j \neq j'} u_{i,jj'}^* \mathcal{G}_k(S_{ij}, S_{ij'}, t) \\ &\quad + \omega_k^{-1} \frac{1}{n} \sum_{i=1}^n \frac{1}{M_{x,i}} \sum_{j \neq j'} u_{i,jj'}^* \frac{K_{h_R}(S_{ij'} - t) \psi_k(S_{ij})}{f_S(S_{ij}) f_S(t)} \\ &\quad + O_p[h_R^2 + (nh_R)^{-1/2} \{h_R + \delta_{n2}(h_R)\}], \\ \hat{\omega}_k - \omega_k &= \frac{1}{n} \sum_{i=1}^n \frac{1}{M_{x,i}} \sum_{j' \neq j} u_{i,jj'}^* \frac{\psi_k(S_{ij}) \psi_k(S_{ij'})}{f_S(S_{ij}) f_S(S_{ij'})} + O_p[h_R^2 + n^{-1/2} \{h_R + \delta_{n2}(h_R)\}], \end{aligned}$$

$k = 1, \dots, q$, where $u_{i,jj'}^* = W_{ij}W_{ij'} - R(S_{ij}, S_{ij'}), M_{x,i} = m_{x,i}(m_{x,i} - 1)$,

$$\mathcal{G}_k(s_1, s_2, s_3) = \sum_{\substack{k'=1 \\ k' \neq k}}^q \frac{\omega_{k'} \psi_{k'}(s_3)}{(\omega_k - \omega_{k'}) \omega_k} \times \left\{ \frac{\psi_k(s_1) \psi_{k'}(s_2)}{f_S(s_1) f_S(s_2)} \right\} - \omega_k^{-1} \psi_k(s_3) \left\{ \frac{\psi_k(s_1) \psi_k(s_2)}{f_S(s_1) f_S(s_2)} \right\}.$$

Proof The asymptotic expansion for $\hat{\psi}_k(t) - \psi_k(t)$ is a direct result of Lemma S.3.1 in Li et al. (2013) by letting $\mu(t) = 0$, and the asymptotic expansion for $\hat{\omega}_k - \omega_k$ is on page 3349 in Li and Hsing (2010). \blacksquare

A.2 The Proof for Theorem 1

Assuming both $X(t)$ and $Y(t)$ have been centered so that $\beta_0 = 0$, we have

$$\sqrt{n}(\hat{\beta}_1 - \beta_1) = \left\{ \frac{1}{n} \sum_{i=1}^n \sum_{j=1}^{m_{y,i}} \hat{X}_i^2(T_{ij}) \right\}^{-1} \left(\frac{1}{\sqrt{n}} \sum_{i=1}^n \sum_{j=1}^{m_{y,i}} \hat{X}_i(T_{ij}) [\{X_i(T_{ij}) - \hat{X}_i(T_{ij})\} \beta_1 + \epsilon_i(T_{ij})] \right).$$

By (14), the denominator of the expression above is

$$\begin{aligned} \frac{1}{n} \sum_{i=1}^n \sum_{j=1}^{m_{y,i}} \hat{X}_i^2(T_{ij}) &= \frac{1}{n} \sum_{i=1}^n \sum_{j=1}^{m_{y,i}} \{\hat{X}_i^2(T_{ij}) - \tilde{X}_i^2(T_{ij})\} + \frac{1}{n} \sum_{i=1}^n \sum_{j=1}^{m_{y,i}} \tilde{X}_i^2(T_{ij}) \\ &= \frac{1}{n} \sum_{i=1}^n \tilde{\mathbf{X}}_{*i}^T \tilde{\mathbf{X}}_{*i} + o_p(1) \\ &\xrightarrow{p} \gamma_x, \end{aligned} \tag{A.3}$$

where $\gamma_x = E(\tilde{\mathbf{X}}_{*i}^T \tilde{\mathbf{X}}_{*i})$ as defined in (15). Define

$$\begin{aligned} \Delta_n &= \frac{1}{\sqrt{n}} \sum_{i=1}^n \sum_{j=1}^{m_{y,i}} \hat{X}_i(T_{ij}) [\{X_i(T_{ij}) - \hat{X}_i(T_{ij})\} \beta_1 + \epsilon_i(T_{ij})] \\ &\quad - \frac{1}{\sqrt{n}} \sum_{i=1}^n \sum_{j=1}^{m_{y,i}} \tilde{X}_i(T_{ij}) [\{X_i(T_{ij}) - \tilde{X}_i(T_{ij})\} \beta_1 + \epsilon_i(T_{ij})] \\ &= \frac{1}{\sqrt{n}} \hat{\mathbf{X}}_*^T \left\{ (\mathbf{X}_* - \hat{\mathbf{X}}_*) \beta_1 + \boldsymbol{\epsilon} \right\} - \frac{1}{\sqrt{n}} \tilde{\mathbf{X}}_*^T \left\{ (\mathbf{X}_* - \tilde{\mathbf{X}}_*) \beta_1 + \boldsymbol{\epsilon} \right\} \\ &= \mathcal{R}_{1,n} + \mathcal{R}_{2,n} + \mathcal{R}_{3,n} + \mathcal{R}_{4,n}, \end{aligned} \tag{A.4}$$

where

$$\begin{aligned} \mathcal{R}_{1,n} &= -\beta_1 \frac{1}{\sqrt{n}} \sum_{i=1}^n (\hat{\mathbf{X}}_{*i} - \tilde{\mathbf{X}}_{*i})^T \tilde{\mathbf{X}}_{*i}, \\ \mathcal{R}_{2,n} &= \beta_1 \frac{1}{\sqrt{n}} \sum_{i=1}^n (\hat{\mathbf{X}}_{*i} - \tilde{\mathbf{X}}_{*i})^T (\mathbf{X}_{*i} - \tilde{\mathbf{X}}_{*i}), \end{aligned}$$

$$\begin{aligned}\mathcal{R}_{3,n} &= \frac{1}{\sqrt{n}} \sum_{i=1}^n (\hat{\mathbf{X}}_{*i} - \tilde{\mathbf{X}}_{*i})^T \boldsymbol{\epsilon}_i, \\ \mathcal{R}_{4,n} &= -\beta_1 \frac{1}{\sqrt{n}} \sum_{i=1}^n (\hat{\mathbf{X}}_{*i} - \tilde{\mathbf{X}}_{*i})^T (\hat{\mathbf{X}}_{*i} - \tilde{\mathbf{X}}_{*i}).\end{aligned}$$

Lemma 2 shows that $\mathcal{R}_{1,n} = O_p(1)$ and provides its asymptotic expansion. Following similar derivations, $\mathcal{R}_{2,n}$ has a similar decomposition as (A.6) except that $\tilde{\mathbf{X}}_{*i}$ is replaced by $\mathbf{X}_{*i} - \tilde{\mathbf{X}}_{*i}$. By lengthy derivations similar to Lemma 2 and using the fact $E\{(\mathbf{X}_{*i} - \tilde{\mathbf{X}}_{*i})\mathbf{W}_i^T \mid \mathbf{T}_i, \mathbf{S}_i\} = \mathbf{0}$, we can show $\mathcal{R}_{2,n} = o_p(1)$. By (14) and the fact that $\boldsymbol{\epsilon}_i$ is uncorrelated with \mathbf{W}_i , we have $\mathcal{R}_{3,n} = o_p(1)$. In addition, $\mathcal{R}_{4,n} = O[\sqrt{n} \times \{h_R^4 + \log n/(nh_R) + h_V^4 + (\log n)^2/(nh_V)^2\}] = o(1)$ a.s. under Assumption (C.4). Combining arguments above,

$$\begin{aligned}\sqrt{n}(\hat{\beta}_1 - \beta_1) &= \frac{1}{\gamma_x \sqrt{n}} \sum_{i=1}^n \left(\sum_{j=1}^{m_{y,i}} \tilde{X}_i(T_{ij}) [\{X_i(T_{ij}) - \tilde{X}_i(T_{ij})\} \beta_1 + \epsilon_i(T_{ij})] \right. \\ &\quad \left. + \frac{\beta_1}{M_{x,i}} \sum_{j \neq j'} u_{i,jj'}^* \mathcal{A}(S_{ij}, S_{i'j'}) \right) + o_p(1) \\ &:= \frac{1}{\gamma_x \sqrt{n}} \sum_{i=1}^n \left(\mathcal{E}_{i1} + \beta_1 \mathcal{E}_{i2} + \beta_1 \mathcal{E}_{i3} \right) + o_p(1),\end{aligned}$$

where $\mathcal{E}_{i1} = \sum_{j=1}^{m_{y,i}} \tilde{X}_i(T_{ij}) \epsilon_i(T_{ij})$, $\mathcal{E}_{i2} = \sum_{j=1}^{m_{y,i}} \tilde{X}_i(T_{ij}) \{X_i(T_{ij}) - \tilde{X}_i(T_{ij})\}$, and $\mathcal{E}_{i3} = \frac{1}{M_{x,i}} \sum_{j \neq j'} u_{i,jj'}^* \mathcal{A}(S_{ij}, S_{i'j'})$. We can verify $E\{(\mathbf{X}_{*i} - \tilde{\mathbf{X}}_{*i})\mathbf{W}_i^T \mid \mathbf{T}_i, \mathbf{S}_i\} = \mathbf{0}$, which means $E(\mathcal{E}_{i2}) = \text{tr}[E\{(\mathbf{X}_{*i} - \tilde{\mathbf{X}}_{*i})\mathbf{W}_i^T \Sigma_i^{-1} \Psi_i \Lambda \Psi_{*i}^T\}] = 0$. With that, it follows that $(\mathcal{E}_{i1}, \mathcal{E}_{i2}, \mathcal{E}_{i3})$ are zero-mean and independent across i , and that \mathcal{E}_{i1} is uncorrelated with $(\mathcal{E}_{i2}, \mathcal{E}_{i3})$ because ϵ is independent of X and W . We have

$$\begin{aligned}\gamma_1 &= \text{Var}(\mathcal{E}_{i1}) = E\left\{ \text{tr}(\Psi_{*i} \Lambda \Psi_i^T \Sigma_i^{-1} \Psi_i \Lambda \Psi_{*i}^T \Omega_i) \right\}, \\ \gamma_2 &= \text{Var}(\mathcal{E}_{i2} + \mathcal{E}_{i3}) = \text{Var}\left[\sum_{j=1}^{m_{y,i}} \tilde{X}_i(T_{ij}) \{X_i(T_{ij}) - \tilde{X}_i(T_{ij})\} + \frac{1}{M_{x,i}} \sum_{j \neq j'} u_{i,jj'}^* \mathcal{A}(S_{ij}, S_{i'j'}) \right],\end{aligned}$$

where $\Omega_i = E(\boldsymbol{\epsilon}_i \boldsymbol{\epsilon}_i^T)$, then by the central limit theory

$$\sqrt{n}(\hat{\beta}_1 - \beta_1) \xrightarrow{d} \text{Normal}\{0, (\gamma_1 + \beta_1^2 \gamma_2)/\gamma_x^2\}.$$

Lemma 2 Under assumptions described in Section 4.1,

$$\mathcal{R}_{1,n} = \beta_1 \frac{1}{\sqrt{n}} \left\{ \sum_{i=1}^n \frac{1}{M_{x,i}} \sum_{j \neq j'} u_{i,jj'}^* \mathcal{A}(S_{ij}, S_{i'j'}) \right\} \{1 + o_p(1)\}, \quad (\text{A.5})$$

where $\mathcal{A}(s_1, s_2) = -\sum_{k=1}^4 \mathcal{A}_k(s_1, s_2)$, $\mathcal{A}_k(s_1, s_2)$, $k = 1, \dots, 4$, are defined in (A.8), (A.10), (A.12) and (A.14), respectively.

Proof We can rewrite $\mathcal{R}_{1,n} = -\beta_1(\mathcal{R}_{11,n} + \mathcal{R}_{12,n} + \mathcal{R}_{13,n} + \mathcal{R}_{14,n})$, where

$$\begin{aligned}\mathcal{R}_{11,n} &= \frac{1}{\sqrt{n}} \sum_{i=1}^n \left\{ \left(\widehat{\Psi}_{*i} - \Psi_{*i} \right) \Lambda \Psi_i^T \Sigma_i^{-1} \mathbf{W}_i \right\}^T \widetilde{\mathbf{X}}_{*i}, \\ \mathcal{R}_{12,n} &= \frac{1}{\sqrt{n}} \sum_{i=1}^n \left\{ \widehat{\Psi}_{*i} \left(\widehat{\Lambda} - \Lambda \right) \Psi_i^T \Sigma_i^{-1} \mathbf{W}_i \right\}^T \widetilde{\mathbf{X}}_{*i}, \\ \mathcal{R}_{13,n} &= \frac{1}{\sqrt{n}} \sum_{i=1}^n \left\{ \widehat{\Psi}_{*i} \widehat{\Lambda} \left(\widehat{\Psi}_i^T - \Psi_i^T \right) \Sigma_i^{-1} \mathbf{W}_i \right\}^T \widetilde{\mathbf{X}}_{*i}, \\ \mathcal{R}_{14,n} &= \frac{1}{\sqrt{n}} \sum_{i=1}^n \left\{ \widehat{\Psi}_{*i} \widehat{\Lambda} \widehat{\Psi}_i^T \left(\widehat{\Sigma}_i^{-1} - \Sigma_i^{-1} \right) \mathbf{W}_i \right\}^T \widetilde{\mathbf{X}}_{*i}.\end{aligned}\tag{A.6}$$

Given a time vector $\mathbf{V} = (V_1, \dots, V_m)^T$, define

$$\mathbf{A}_1(s_1, s_2, \mathbf{V}) = \mathcal{G}(s_1, s_2, \mathbf{V}) + \left\{ \frac{K_{h_R}(s_2 - V_1)}{f_S(V_1)}, \dots, \frac{K_{h_R}(s_2 - V_m)}{f_S(V_m)} \right\}^T \mathbf{A}_1^*(s_1) \tag{A.7}$$

where $\mathcal{G}(s_1, s_2, \mathbf{V}) = \{\mathcal{G}_1(s_1, s_2, \mathbf{V}), \dots, \mathcal{G}_q(s_1, s_2, \mathbf{V})\}$, $\mathcal{G}_k(s_1, s_2, \mathbf{V}) = \{\mathcal{G}_k(s_1, s_2, V_1), \dots, \mathcal{G}_k(s_1, s_2, V_m)\}^T$, $\mathcal{G}_k(s_1, s_2, V)$ defined in Lemma 1, and

$$\mathbf{A}_1^*(s_1) = \left\{ \frac{\psi_1(s_1)}{f_S(s_1)\omega_1}, \dots, \frac{\psi_q(s_1)}{f_S(s_1)\omega_q} \right\}.$$

In addition, define

$$\mathcal{A}_1(s_1, s_2) = \text{tr} \left(\mathbf{E} \left(\Lambda \Psi_i^T \Sigma_i^{-1} \Psi_i \Lambda \right) \left[\mathbf{E} \left\{ \Psi_{*i}^T \mathcal{G}(s_1, s_2, \mathbf{T}_i) \right\} + \mathbf{E}(m_{y,i}) \boldsymbol{\psi}(s_2) \mathbf{A}_1^*(s_1) \right] \right). \tag{A.8}$$

By Lemma 1,

$$\begin{aligned}\mathcal{R}_{11,n} &= \frac{1}{\sqrt{n}} \sum_{i=1}^n \mathbf{W}_i^T \Sigma_i^{-1} \Psi_i \Lambda \left(\widehat{\Psi}_{*i} - \Psi_{*i} \right)^T \widetilde{\mathbf{X}}_{*i} \\ &= \frac{1}{\sqrt{n}} \sum_{i=1}^n \mathbf{W}_i^T \Sigma_i^{-1} \Psi_i \Lambda \left\{ \frac{1}{n} \sum_{i'=1}^n \frac{1}{M_{x,i'}} \sum_{l \neq l'} u_{i',ll'}^* \mathbf{A}_1(S_{i'l}, S_{i'l'}, \mathbf{T}_i)^T \right\} \widetilde{\mathbf{X}}_{*i} + O_p\{\zeta_n(h_R)\} \\ &= \frac{1}{\sqrt{n}} \sum_{i'=1}^n \frac{1}{M_{x,i'}} \sum_{l \neq l'} u_{i',ll'}^* \frac{1}{n} \sum_{i=1}^n \mathbf{W}_i^T \Sigma_i^{-1} \Psi_i \Lambda \mathbf{A}_1(S_{i'l}, S_{i'l'}, \mathbf{T}_i)^T \widetilde{\mathbf{X}}_{*i} + O_p\{\zeta_n(h_R)\} \\ &= \left[\frac{1}{\sqrt{n}} \sum_{i'=1}^n \frac{1}{M_{x,i'}} \sum_{l \neq l'} u_{i',ll'}^* \mathbf{E} \left\{ \mathbf{W}_i^T \Sigma_i^{-1} \Psi_i \Lambda \mathbf{A}_1(s_1, s_2, \mathbf{T}_i)^T \widetilde{\mathbf{X}}_{*i} \right\} \Big|_{s_1=S_{i'l}, s_2=S_{i'l'}} \right] \\ &\quad \times \{1 + o_p(1)\} + O_p\{\zeta_n(h_R)\}, \\ &= \left\{ \frac{1}{\sqrt{n}} \sum_{i'=1}^n \frac{1}{M_{x,i'}} \sum_{l \neq l'} u_{i',ll'}^* \mathcal{A}_1(S_{i'l}, S_{i'l'}) \right\} \{1 + o_p(1)\} + O_p\{\zeta_n(h_R)\},\end{aligned}\tag{A.9}$$

and $\zeta_n(h_R) = o(1)$ by (C.4).

Put

$$\mathbf{A}_2(s_1, s_2) = \text{diag} \left\{ \frac{\psi_1(s_1)\psi_1(s_2)}{f_S(s_1)f_S(s_2)}, \dots, \frac{\psi_q(s_1)\psi_q(s_2)}{f_S(s_1)f_S(s_2)} \right\}, \quad (\text{A.10})$$

$$\mathcal{A}_2(s_1, s_2) = \mathbb{E} \left\{ \mathbf{W}_i^T \boldsymbol{\Sigma}_i^{-1} \boldsymbol{\Psi}_i \mathbf{A}_2(s_1, s_2) \boldsymbol{\Psi}_{*i}^T \tilde{\mathbf{X}}_{*i} \right\} = \text{tr} \left\{ \mathbf{A}_2(s_1, s_2) \mathbb{E} \left(\boldsymbol{\Psi}_{*i}^T \boldsymbol{\Psi}_{*i} \boldsymbol{\Lambda} \boldsymbol{\Psi}_i^T \boldsymbol{\Sigma}_i^{-1} \boldsymbol{\Psi}_i \right) \right\},$$

then by Lemma 1 and Condition (C.4),

$$\begin{aligned} \mathcal{R}_{12,n} &= \frac{1}{\sqrt{n}} \sum_{i=1}^n \left\{ \hat{\boldsymbol{\Psi}}_{*i} \left(\hat{\boldsymbol{\Lambda}} - \boldsymbol{\Lambda} \right) \boldsymbol{\Psi}_i^T \boldsymbol{\Sigma}_i^{-1} \mathbf{W}_i \right\}^T \tilde{\mathbf{X}}_{*i} \\ &= \left\{ \frac{1}{\sqrt{n}} \sum_{i=1}^n \mathbf{W}_i^T \boldsymbol{\Sigma}_i^{-1} \boldsymbol{\Psi}_i \frac{1}{n} \sum_{i'=1}^n \frac{1}{M_{x,i'}} \sum_{l \neq l'} u_{i',ll'}^* \mathbf{A}_2(S_{i'l}, S_{i'l'}) \boldsymbol{\Psi}_{*i}^T \tilde{\mathbf{X}}_{*i} \right\} \{1 + o_p(1)\} \\ &= \left\{ \frac{1}{\sqrt{n}} \sum_{i'=1}^n \frac{1}{M_{x,i'}} \sum_{l' \neq l} u_{i',ll'}^* \frac{1}{n} \sum_{i=1}^n \mathbf{W}_i^T \boldsymbol{\Sigma}_i^{-1} \boldsymbol{\Psi}_i \mathbf{A}_2(S_{i'l}, S_{i'l'}) \boldsymbol{\Psi}_{*i}^T \tilde{\mathbf{X}}_{*i} \right\} \{1 + o_p(1)\} \\ &= \left\{ \frac{1}{\sqrt{n}} \sum_{i'=1}^n \frac{1}{M_{x,i'}} \sum_{l' \neq l} u_{i',ll'}^* \mathcal{A}_2(S_{i'l}, S_{i'l'}) \right\} \{1 + o_p(1)\}. \end{aligned} \quad (\text{A.11})$$

Next, define

$$\begin{aligned} \mathcal{A}_3(s_1, s_2) &= \text{tr} \left[\mathbb{E} \left\{ \boldsymbol{\Lambda} \mathcal{G}(s_1, s_2, \mathbf{S}_i)^T \boldsymbol{\Sigma}_i^{-1} \boldsymbol{\Psi}_i \boldsymbol{\Lambda} \right\} \mathbb{E} \left(\boldsymbol{\Psi}_{*i}^T \boldsymbol{\Psi}_{*i} \right) \right] \\ &\quad + \text{tr} \left[f_S^{-1}(s_1) \boldsymbol{\psi}(s_1) \mathbb{E} \left\{ \sum_{j=1}^{m_{x,i}} \mathbb{E} \left(\mathbf{e}_j^T \boldsymbol{\Sigma}_i^{-1} \boldsymbol{\Psi}_i \mid S_{ij} = s_2, m_{x,i} \right) \right\} \boldsymbol{\Lambda} \mathbb{E} \left(\boldsymbol{\Psi}_{*i}^T \boldsymbol{\Psi}_{*i} \right) \right]. \end{aligned} \quad (\text{A.12})$$

where $\mathcal{G}(s_1, s_2, \mathbf{T}_i)$ is defined in (A.7), and \mathbf{e}_j is a directional vector of length $m_{x,i}$ with all elements being zero, except that the j th is 1. Following similar derivations as in (A.9), we have

$$\begin{aligned} \mathcal{R}_{13,n} &= \frac{1}{\sqrt{n}} \sum_{i=1}^n \mathbf{W}_i^T \boldsymbol{\Sigma}_i^{-1} \left(\hat{\boldsymbol{\Psi}}_i - \boldsymbol{\Psi}_i \right) \hat{\boldsymbol{\Lambda}} \hat{\boldsymbol{\Psi}}_{*i}^T \tilde{\mathbf{X}}_{*i} \\ &= \left\{ \frac{1}{\sqrt{n}} \sum_{i=1}^n \mathbf{W}_i^T \boldsymbol{\Sigma}_i^{-1} \frac{1}{n} \sum_{i'=1}^n \frac{1}{M_{x,i'}} \sum_{l \neq l'} u_{i',ll'}^* \mathbf{A}_1(S_{i'l}, S_{i'l'}, \mathbf{S}_i) \boldsymbol{\Lambda} \boldsymbol{\Psi}_{*i}^T \tilde{\mathbf{X}}_{*i} \right\} \{1 + o_p(1)\} \\ &= \left\{ \frac{1}{\sqrt{n}} \sum_{i'=1}^n \frac{1}{M_{x,i'}} \sum_{l' \neq l} u_{i',ll'}^* \frac{1}{n} \sum_{i=1}^n \mathbf{W}_i^T \boldsymbol{\Sigma}_i^{-1} \mathbf{A}_1(S_{i'l}, S_{i'l'}, \mathbf{S}_i) \boldsymbol{\Lambda} \boldsymbol{\Psi}_{*i}^T \tilde{\mathbf{X}}_{*i} \right\} \{1 + o_p(1)\} \\ &= \left[\frac{1}{\sqrt{n}} \sum_{i'=1}^n \frac{1}{M_{x,i'}} \sum_{l' \neq l} u_{i',ll'}^* \mathbb{E} \left\{ \mathbf{W}_i^T \boldsymbol{\Sigma}_i^{-1} \mathbf{A}_1(s_1, s_2, \mathbf{S}_i) \boldsymbol{\Lambda} \boldsymbol{\Psi}_{*i}^T \tilde{\mathbf{X}}_{*i} \right\} \mid s_1 = S_{i'l}, s_2 = S_{i'l'} \right] \\ &\quad \times \{1 + o_p(1)\} \\ &= \left\{ \frac{1}{\sqrt{n}} \sum_{i'=1}^n \frac{1}{M_{x,i'}} \sum_{l' \neq l} u_{i',ll'}^* \mathcal{A}_3(S_{i'l}, S_{i'l'}) \right\} \{1 + o_p(1)\}. \end{aligned} \quad (\text{A.13})$$

The last equation above follows because

$$\begin{aligned}
 & \mathbb{E} \left\{ \mathbf{W}_i^T \boldsymbol{\Sigma}_i^{-1} \mathbf{A}_1(s_1, s_2, \mathbf{S}_i) \boldsymbol{\Lambda} \boldsymbol{\Psi}_{*i}^T \tilde{\mathbf{X}}_{*i} \right\} \\
 &= \text{tr} \left[\mathbb{E} \left\{ \boldsymbol{\Lambda} \mathbf{A}_1(s_1, s_2, \mathbf{S}_i)^T \boldsymbol{\Sigma}_i^{-1} \boldsymbol{\Psi}_i \boldsymbol{\Lambda} \boldsymbol{\Psi}_{*i}^T \boldsymbol{\Psi}_{*i} \right\} \right] \\
 &= \text{tr} \left[\mathbb{E} \left\{ \boldsymbol{\Lambda} \mathcal{G}(s_1, s_2, \mathbf{S}_i)^T \boldsymbol{\Sigma}_i^{-1} \boldsymbol{\Psi}_i \boldsymbol{\Lambda} \right\} \mathbb{E} \left(\boldsymbol{\Psi}_{*i}^T \boldsymbol{\Psi}_{*i} \right) \right] \\
 &+ \text{tr} \left[f_S^{-1}(s_1) \boldsymbol{\psi}(s_1)^T \mathbb{E} \left\{ \sum_{j=1}^{m_{x,i}} \mathbb{E} \left(\mathbf{e}_j^T \boldsymbol{\Sigma}_i^{-1} \boldsymbol{\Psi}_i \mid S_{ij} = s_2, m_{x,i} \right) \right\} \boldsymbol{\Lambda} \mathbb{E} \left(\boldsymbol{\Psi}_{*i}^T \boldsymbol{\Psi}_{*i} \right) \right] + O(h_R^2).
 \end{aligned}$$

For the last term (A.6),

$$\frac{1}{\sqrt{n}} \sum_{i=1}^n \left\{ \hat{\boldsymbol{\Psi}}_{*i} \hat{\boldsymbol{\Lambda}} \hat{\boldsymbol{\Psi}}_i^T \left(\hat{\boldsymbol{\Sigma}}_i^{-1} - \boldsymbol{\Sigma}_i^{-1} \right) \mathbf{W}_i \right\}^T \tilde{\mathbf{X}}_{*i} = \frac{1}{\sqrt{n}} \sum_{i=1}^n \mathbf{W}_i^T \left(\hat{\boldsymbol{\Sigma}}_i^{-1} - \boldsymbol{\Sigma}_i^{-1} \right) \hat{\boldsymbol{\Psi}}_i \hat{\boldsymbol{\Lambda}} \hat{\boldsymbol{\Psi}}_{*i}^T \tilde{\mathbf{X}}_{*i}.$$

Finally, define

$$\begin{aligned}
 \mathcal{A}_4(s_1, s_2) &= -2 \text{tr} \left[\mathbb{E} \left\{ \boldsymbol{\Sigma}_i^{-1} \boldsymbol{\Psi}_i \boldsymbol{\Lambda} \boldsymbol{\Psi}_{*i}^T \boldsymbol{\Psi}_{*i} \boldsymbol{\Lambda} \boldsymbol{\Psi}_i^T \boldsymbol{\Sigma}_i^{-1} \boldsymbol{\Psi}_i \boldsymbol{\Lambda} \mathcal{G}(s_1, s_2, \mathbf{S}_i)^T \right\} \right] \\
 &- 2 \mathbb{E} \left[\sum_{j=1}^{m_{x,i}} \mathbb{E} \left\{ \mathbf{e}_j^T \boldsymbol{\Sigma}_i^{-1} \boldsymbol{\Psi}_i^T \boldsymbol{\Lambda} \mathbb{E} \left(\boldsymbol{\Psi}_{*i}^T \boldsymbol{\Psi}_{*i} \right) \boldsymbol{\Lambda} \boldsymbol{\Psi}_i^T \boldsymbol{\Sigma}_i^{-1} \boldsymbol{\Psi}_i \mid S_{ij} = s_2, m_{x,i} \right\} \right] \frac{\boldsymbol{\psi}(s_1)}{f_S(s_1)} \\
 &- \text{tr} \left[\mathbb{E} \left\{ \boldsymbol{\Sigma}_i^{-1} \boldsymbol{\Psi}_i \boldsymbol{\Lambda} \boldsymbol{\Psi}_{*i}^T \boldsymbol{\Psi}_{*i} \boldsymbol{\Lambda} \boldsymbol{\Psi}_i^T \boldsymbol{\Sigma}_i^{-1} \boldsymbol{\Psi}_i \mathbf{A}_2(s_1, s_2) \boldsymbol{\Psi}_i^T \right\} \right]. \tag{A.14}
 \end{aligned}$$

By matrix taylor expansion, $\hat{\boldsymbol{\Sigma}}_i^{-1} = \boldsymbol{\Sigma}_i^{-1} - \boldsymbol{\Sigma}_i^{-1} \left(\hat{\boldsymbol{\Sigma}}_i - \boldsymbol{\Sigma}_i \right) \boldsymbol{\Sigma}_i^{-1} \{1 + o_p(1)\}$. Thus, by Lemma 1 and using similar calculations as for $\mathcal{R}_{11,n}$, we have

$$\begin{aligned}
 \mathcal{R}_{14,n} &= \frac{1}{\sqrt{n}} \sum_{i=1}^n \left\{ \hat{\boldsymbol{\Psi}}_{*i} \hat{\boldsymbol{\Lambda}} \hat{\boldsymbol{\Psi}}_i^T \left(\hat{\boldsymbol{\Sigma}}_i^{-1} - \boldsymbol{\Sigma}_i^{-1} \right) \mathbf{W}_i \right\}^T \tilde{\mathbf{X}}_{*i} \\
 &= \left\{ \frac{1}{\sqrt{n}} \sum_{i=1}^n \mathbf{W}_i^T \boldsymbol{\Sigma}_i^{-1} \left(\boldsymbol{\Sigma}_i - \hat{\boldsymbol{\Sigma}}_i \right) \boldsymbol{\Sigma}_i^{-1} \boldsymbol{\Psi}_i \boldsymbol{\Lambda} \boldsymbol{\Psi}_{*i}^T \tilde{\mathbf{X}}_{*i} \right\} \{1 + o_p(1)\} \\
 &= \left\{ \frac{1}{\sqrt{n}} \sum_{i=1}^n \mathbf{W}_i^T \boldsymbol{\Sigma}_i^{-1} \left(\boldsymbol{\Psi}_i \boldsymbol{\Lambda} \boldsymbol{\Psi}_i^T - \hat{\boldsymbol{\Psi}}_i \hat{\boldsymbol{\Lambda}} \hat{\boldsymbol{\Psi}}_i^T \right) \boldsymbol{\Sigma}_i^{-1} \boldsymbol{\Psi}_i \boldsymbol{\Lambda} \boldsymbol{\Psi}_{*i}^T \tilde{\mathbf{X}}_{*i} \right\} \{1 + o_p(1)\} \\
 &+ (\sigma_u^2 - \hat{\sigma}_u^2) \left\{ \frac{1}{\sqrt{n}} \sum_{i=1}^n \mathbf{W}_i^T \boldsymbol{\Sigma}_i^{-2} \boldsymbol{\Psi}_i \boldsymbol{\Lambda} \boldsymbol{\Psi}_{*i}^T \tilde{\mathbf{X}}_{*i} \right\} \{1 + o_p(1)\} \\
 &= - \left[\frac{1}{\sqrt{n}} \sum_{i=1}^n \mathbf{W}_i^T \boldsymbol{\Sigma}_i^{-1} \left\{ (\hat{\boldsymbol{\Psi}}_i - \boldsymbol{\Psi}_i) \boldsymbol{\Lambda} \boldsymbol{\Psi}_i^T + \boldsymbol{\Psi}_i (\hat{\boldsymbol{\Lambda}} - \boldsymbol{\Lambda}) \boldsymbol{\Psi}_i^T + \boldsymbol{\Psi}_i \boldsymbol{\Lambda} (\hat{\boldsymbol{\Psi}}_i - \boldsymbol{\Psi}_i)^T \right\} \right. \\
 &\quad \left. \times \boldsymbol{\Sigma}_i^{-1} \boldsymbol{\Psi}_i \boldsymbol{\Lambda} \boldsymbol{\Psi}_{*i}^T \tilde{\mathbf{X}}_{*i} \right] \{1 + o_p(1)\} + o_p(1) \\
 &= - \left[\frac{1}{\sqrt{n}} \sum_{i=1}^n \mathbf{W}_i^T \boldsymbol{\Sigma}_i^{-1} \frac{1}{n} \sum_{i'=1}^n \frac{1}{M_{x,i'}} \sum_{l \neq l'} u_{i',l'}^* \left\{ \mathbf{A}_1(S_{i'l}, S_{i'l'}, \mathbf{S}_i) \boldsymbol{\Lambda} \boldsymbol{\Psi}_i^T + \boldsymbol{\Psi}_i \mathbf{A}_2(S_{i'l}, S_{i'l'}) \boldsymbol{\Psi}_i^T \right. \right. \\
 &\quad \left. \left. + \boldsymbol{\Psi}_i \boldsymbol{\Lambda} \mathbf{A}_1(S_{i'l}, S_{i'l'}, \mathbf{S}_i)^T \right\} \boldsymbol{\Sigma}_i^{-1} \boldsymbol{\Psi}_i \boldsymbol{\Lambda} \boldsymbol{\Psi}_{*i}^T \tilde{\mathbf{X}}_{*i} \right] \{1 + o_p(1)\} + o_p(1)
 \end{aligned}$$

$$= \left\{ \frac{1}{\sqrt{n}} \sum_{i'=1}^n \frac{1}{M_{x,i'}} \sum_{l' \neq l} u_{i',l'}^* \mathcal{A}_4(S_{i'l}, S_{i'l'}) \right\} \{1 + o_p(1)\} + o_p(1), \quad (\text{A.15})$$

where the last equation is due to that

$$\begin{aligned} & -E \left[\mathbf{W}_i^T \Sigma_i^{-1} \{ \mathbf{A}_1(s_1, s_2, \mathbf{S}_i) \mathbf{\Lambda} \Psi_i^T + \Psi_i \mathbf{A}_2(s_1, s_2) \Psi_i^T + \Psi_i \mathbf{\Lambda} \mathbf{A}_1(s_1, s_2, \mathbf{S}_i)^T \} \Sigma_i^{-1} \Psi_i \mathbf{\Lambda} \Psi_{*i}^T \tilde{\mathbf{X}}_{*i} \right] \\ & = \mathcal{A}_4(s_1, s_2) + O(h_R^2). \end{aligned}$$

The asymptotic expansion of \mathcal{R}_{1n} provided in the lemma is proven by combining (A.9), (A.11), (A.13) and (A.15). ■

A.3 The Proof for Theorem 2

Under the simplified setting X_i are mean zero random process, by simple algebra we have

$$\hat{\beta}_1(t) = \frac{S_2(t)R_0(t) - S_1(t)R_1(t)}{S_2(t)S_0(t) - S_1^2(t)},$$

where

$$\begin{aligned} S_r(t) &= \frac{1}{n} \sum_{i=1}^n \sum_{j=1}^{m_{y,i}} \hat{X}_i^2(T_{ij}) K_h(T_{ij} - t) \{(T_{ij} - t)/h\}^r, \quad r = 0, 1, 2, \\ R_r(t) &= \frac{1}{n} \sum_{i=1}^n \sum_{j=1}^{m_{y,i}} \hat{X}_i(T_{ij}) Y_{ij} K_h(T_{ij} - t) \{(T_{ij} - t)/h\}^r, \quad r = 0, 1. \end{aligned}$$

Denote $R_r^*(t) = R_r(t) - S_r(t)\beta_1(t) - S_{r+1}(t)h\beta_1'(t)$, $r = 0, 1$, then

$$\hat{\beta}_1(t) - \beta_1(t) = \frac{S_2(t)R_0^*(t) - S_1(t)R_1^*(t)}{S_2(t)S_0(t) - S_1^2(t)}.$$

By (14) and using the general result from Lemma 2 in Li and Hsing (2010),

$$\begin{aligned} S_0(t) &= \frac{1}{n} \sum_{i=1}^n \sum_{j=1}^{m_{y,i}} \tilde{X}_i^2(T_{ij}) K_h(T_{ij} - t) + O\{h_R^2 + h_V^2 + \sqrt{\log n/(nh_R)} + \log n/(nh_V)\} \\ &= \bar{m}_y f_T(t) \Gamma_x(t) + O_p\{h^2 + \sqrt{\log n/(nh)} + h_R^2 + h_V^2 + \sqrt{\log n/(nh_R)} + \log n/(nh_V)\}, \end{aligned}$$

where $\Gamma_x(t) = \text{Var}\{\tilde{X}_i(t)\} = \boldsymbol{\psi}^T(t) \mathbf{\Lambda} E(\Psi_i^T \Sigma_i^{-1} \Psi_i) \mathbf{\Lambda} \boldsymbol{\psi}(t)$ as defined in the theorem. Similarly, $S_1(t) = \{\Gamma_x'(t) f_T(t) + \Gamma_x(t) f_T'(t)\} \bar{m}_y \sigma_K^2 h + O_p\{h^3 + \sqrt{\log n/(nh)} + h_R^2 + h_V^2 + \sqrt{\log n/(nh_R)} + \log n/(nh_V)\}$ and $S_2(t) = \bar{m}_y \Gamma_x(t) f_T(t) \sigma_K^2 + O_p\{h^2 + \sqrt{\log n/(nh)} + h_R^2 + h_V^2 + \sqrt{\log n/(nh_R)} + \log n/(nh_V)\}$.

Next, we decompose R_r^* as

$$R_r^*(t) = \frac{1}{n} \sum_{i=1}^n \sum_{j=1}^{m_{y,i}} \hat{X}_i(T_{ij}) \left\{ Y_{ij} - \hat{X}_i(T_{ij}) \beta_1(t) - \hat{X}_i(T_{ij}) (T_{ij} - t) \beta_1'(t) \right\}$$

$$\begin{aligned}
 & \times K_h(T_{ij} - t) \{(T_{ij} - t)/h\}^r \\
 & = \sum_{k=1}^6 R_{r,k}^*(t),
 \end{aligned} \tag{A.16}$$

where

$$\begin{aligned}
 R_{r,1}^*(t) &= \frac{1}{n} \sum_{i=1}^n \sum_{j=1}^{m_{y,i}} \hat{X}_i^2(T_{ij}) \{\beta_1(T_{ij}) - \beta_1(t) - (T_{ij} - t)\beta_1'(t)\} K_h(T_{ij} - t) \{(T_{ij} - t)/h\}^r, \\
 R_{r,2}^*(t) &= \frac{1}{n} \sum_{i=1}^n \sum_{j=1}^{m_{y,i}} \tilde{X}_i(T_{ij}) \{\beta_1(T_{ij}) X_i(T_{ij}) - \beta_1(T_{ij}) \tilde{X}_i(T_{ij}) + \epsilon_i(T_{ij})\} K_h(T_{ij} - t) \{(T_{ij} - t)/h\}^r, \\
 R_{r,3}^*(t) &= \frac{1}{n} \sum_{i=1}^n \sum_{j=1}^{m_{y,i}} \{\tilde{X}_i(T_{ij}) - \hat{X}_i(T_{ij})\} \tilde{X}_i(T_{ij}) \beta_1(T_{ij}) K_h(T_{ij} - t) \{(T_{ij} - t)/h\}^r, \\
 R_{r,4}^*(t) &= \frac{1}{n} \sum_{i=1}^n \sum_{j=1}^{m_{y,i}} \{\hat{X}_i(T_{ij}) - \tilde{X}_i(T_{ij})\} \epsilon_i(T_{ij}) K_h(T_{ij} - t) \{(T_{ij} - t)/h\}^r, \\
 R_{r,5}^*(t) &= \frac{1}{n} \sum_{i=1}^n \sum_{j=1}^{m_{y,i}} \{\hat{X}_i(T_{ij}) - \tilde{X}_i(T_{ij})\} \{X_i(T_{ij}) - \tilde{X}_i(T_{ij})\} \beta_1(T_{ij}) K_h(T_{ij} - t) \{(T_{ij} - t)/h\}^r, \\
 R_{r,6}^*(t) &= \frac{1}{n} \sum_{i=1}^n \sum_{j=1}^{m_{y,i}} \{\hat{X}_i(T_{ij}) - \tilde{X}_i(T_{ij})\} \{\tilde{X}_i(T_{ij}) - \hat{X}_i(T_{ij})\} \beta_1(T_{ij}) K_h(T_{ij} - t) \{(T_{ij} - t)/h\}^r.
 \end{aligned}$$

By (14) and previous results for $S_r(t)$, using some straightforward calculations and the fact that $K_h(T_{ij} - t) = 0$ if $|T_{ij} - t| > h$,

$$\begin{aligned}
 R_{0,1}^*(t) &= \frac{1}{n} \sum_{i=1}^n \sum_{j=1}^{m_{y,i}} \hat{X}_i^2(T_{ij}) \{\beta_1(T_{ij}) - \beta_1(t) - (T_{ij} - t)\beta_1'(t)\} K_h(T_{ij} - t) \\
 &= \frac{1}{2} \beta_1^{(2)}(t) h^2 \left[\frac{1}{n} \sum_{i=1}^n \sum_{j=1}^{m_{y,i}} \hat{X}_i^2(T_{ij}) K_h(T_{ij} - t) \{(T_{ij} - t)/h\}^2 \right] \{1 + O(h)\} \\
 &= \frac{1}{2} \beta_1^{(2)}(t) h^2 \bar{m}_y f_T(t) \Gamma_x(t) \sigma_K^2 [1 + O_p\{h + \sqrt{\log n/(nh)} + h_R^2 \\
 &\quad + h_V^2 + \sqrt{\log n/(nh_R)} + \log n/(nh_V)\}].
 \end{aligned}$$

By similar calculations, $R_{1,1}^*(t) = O_p[h^3 + h^2 \sqrt{\log n/(nh)} + h^2 \{h_R^2 + h_V^2 + \sqrt{\log n/(nh_R)} + \log n/(nh_V)\}]$ is of order $o_p\{(nh)^{-1/2}\}$ by conditions (C.4) and (C.7). In addition, it follows that $R_{r,4}^*(t)$ and $R_{r,5}^*(t)$ are both of order $O_p([h_R^2 + h_V^2 + \{\log n/(nh_R)\}^{1/2} + \log n/(nh_V)] \times \{\log n/(nh)\}^{1/2})$, which is $o_p\{(nh)^{-1/2}\}$, and $R_{r,6}^*(t) = h_R^4 + h_V^4 + \log n/(nh_R) + (\log n)^2/(nh_V)^2] = o_p\{(nh)^{-1/2}\}$ under Condition (C.4), for both $r = 0, 1$.

Define

$$\mathbf{K}_{r,*i}(t) = \text{diag} \left[K_h(T_{i1} - t) \{(T_{i1} - t)/h\}^r, \dots, K_h(T_{im_{y,i}} - t) \{(T_{im_{y,i}} - t)/h\}^r \right],$$

$$\mathbf{K}_i^\dagger(s, \mathbf{T}_i) = \left\{ \frac{K_{h_R}(s - T_{i1})}{f_S(T_{i1})}, \dots, \frac{K_{h_R}(s - T_{im_{y,i}})}{f_S(T_{im_{y,i}})} \right\}^\top,$$

$$\boldsymbol{\beta}_{*i} = \text{diag} \left\{ \beta_1(T_{i1}), \dots, \beta_1(T_{im_{y,i}}) \right\},$$

then we have

$$R_{r,3}^*(t) = - \sum_{k=1}^4 R_{r,3k}^*(t) \quad (\text{A.17})$$

where

$$\begin{aligned} R_{r,31}^*(t) &= \frac{1}{n} \sum_{i=1}^n \left\{ \left(\widehat{\boldsymbol{\Psi}}_{*i} - \boldsymbol{\Psi}_{*i} \right) \boldsymbol{\Lambda} \boldsymbol{\Psi}_i^\top \boldsymbol{\Sigma}_i^{-1} \mathbf{W}_i \right\}^\top \mathbf{K}_{r,*i}(t) \boldsymbol{\beta}_{*i} \widetilde{\mathbf{X}}_{*i}, \\ R_{r,32}^*(t) &= \frac{1}{n} \sum_{i=1}^n \left\{ \widehat{\boldsymbol{\Psi}}_{*i} \left(\widehat{\boldsymbol{\Lambda}} - \boldsymbol{\Lambda} \right) \boldsymbol{\Psi}_i^\top \boldsymbol{\Sigma}_i^{-1} \mathbf{W}_i \right\}^\top \mathbf{K}_{r,*i}(t) \boldsymbol{\beta}_{*i} \widetilde{\mathbf{X}}_{*i}, \\ R_{r,33}^*(t) &= \frac{1}{n} \sum_{i=1}^n \left\{ \widehat{\boldsymbol{\Psi}}_{*i} \widehat{\boldsymbol{\Lambda}} \left(\widehat{\boldsymbol{\Psi}}_i^\top - \boldsymbol{\Psi}_i^\top \right) \boldsymbol{\Sigma}_i^{-1} \mathbf{W}_i \right\}^\top \mathbf{K}_{r,*i}(t) \boldsymbol{\beta}_{*i} \widetilde{\mathbf{X}}_{*i}, \\ R_{r,34}^*(t) &= \frac{1}{n} \sum_{i=1}^n \left\{ \widehat{\boldsymbol{\Psi}}_{*i} \widehat{\boldsymbol{\Lambda}} \widehat{\boldsymbol{\Psi}}_i^\top \left(\widehat{\boldsymbol{\Sigma}}_i^{-1} - \boldsymbol{\Sigma}_i^{-1} \right) \mathbf{W}_i \right\}^\top \mathbf{K}_{r,*i}(t) \boldsymbol{\beta}_{*i} \widetilde{\mathbf{X}}_{*i}. \end{aligned}$$

Let $\mathbf{A}_1(s_1, s_2, \mathbf{T}_i)$ be defined as (A.7), using derivations similar to (A.9), by (C.4) we have

$$\begin{aligned} R_{r,31}^*(t) &= \left[\frac{1}{n} \sum_{i=1}^n \mathbf{W}_i^\top \boldsymbol{\Sigma}_i^{-1} \boldsymbol{\Psi}_i \boldsymbol{\Lambda} \left\{ \frac{1}{n} \sum_{i'=1}^n \frac{1}{M_{x,i'}} \sum_{l \neq l'} u_{i',l'}^* \mathbf{A}_1(S_{i'l}, S_{i'l'}, \mathbf{T}_i)^\top \right\} \mathbf{K}_{r,*i}(t) \boldsymbol{\beta}_{*i} \widetilde{\mathbf{X}}_{*i} \right] \\ &\quad \times \{1 + o_p(1)\} \\ &= \left[\frac{1}{n} \sum_{i'=1}^n \frac{1}{M_{x,i'}} \sum_{l \neq l'} u_{i',l'}^* \left\{ \frac{1}{n} \sum_{i=1}^n \mathbf{W}_i^\top \boldsymbol{\Sigma}_i^{-1} \boldsymbol{\Psi}_i \boldsymbol{\Lambda} \mathbf{A}_1(S_{i'l}, S_{i'l'}, \mathbf{T}_i)^\top \mathbf{K}_{r,*i}(t) \boldsymbol{\beta}_{*i} \widetilde{\mathbf{X}}_{*i} \right\} \right] \\ &\quad \times \{1 + o_p(1)\} \\ &= \left[\frac{1}{n} \sum_{i'=1}^n \frac{1}{M_{x,i'}} \sum_{l \neq l'} u_{i',l'}^* \left\{ \frac{1}{n} \sum_{i=1}^n \mathbf{W}_i^\top \boldsymbol{\Sigma}_i^{-1} \boldsymbol{\Psi}_i f_S^{-1}(S_{i'l}) \boldsymbol{\psi}(S_{i'l}) \mathbf{K}_i^\dagger(S_{i'l'}, \mathbf{T}_i)^\top \right. \right. \\ &\quad \left. \left. \times \mathbf{K}_{r,*i}(t) \boldsymbol{\beta}_{*i} \widetilde{\mathbf{X}}_{*i} \right\} + O_p(n^{-1/2}) \right] \times \{1 + o_p(1)\}. \end{aligned}$$

Define

$$\mathcal{Q}(s, t) = \boldsymbol{\psi}^\top(t) \boldsymbol{\Lambda} \mathbf{E}(\boldsymbol{\Psi}_i^\top \boldsymbol{\Sigma}_i^{-1} \boldsymbol{\Psi}_i) \boldsymbol{\psi}(s) f_T(t) / \{f_S(s) f_S(t)\}, \quad (\text{A.18})$$

then

$$\begin{aligned} &\mathbf{E} \left\{ \mathbf{W}_i^\top \boldsymbol{\Sigma}_i^{-1} \boldsymbol{\Psi}_i f_S^{-1}(s_1) \boldsymbol{\psi}(s_1) \mathbf{K}_i^\dagger(s_2, \mathbf{T}_i)^\top \mathbf{K}_{r,*i}(t) \boldsymbol{\beta}_{*i} \widetilde{\mathbf{X}}_{*i} \right\} \\ &= \text{tr} \left[\mathbf{E} \left\{ \boldsymbol{\Psi}_{*i} \boldsymbol{\Lambda} \boldsymbol{\Psi}_i^\top \boldsymbol{\Sigma}_i^{-1} \boldsymbol{\Psi}_i f_S^{-1}(s_1) \boldsymbol{\psi}(s_1) \mathbf{K}_i^\dagger(s_2, \mathbf{T}_i)^\top \mathbf{K}_{r,*i}(t) \boldsymbol{\beta}_{*i} \right\} \right] \end{aligned}$$

$$\begin{aligned}
 &= \mathbb{E} \left[\sum_{j=1}^{m_{y,i}} \boldsymbol{\psi}^T(T_{ij}) \boldsymbol{\Lambda} \boldsymbol{\Psi}_i^T \boldsymbol{\Sigma}_i^{-1} \boldsymbol{\Psi}_i \boldsymbol{\psi}(s_1) \frac{K_{h_R}(s_2 - T_{ij})}{f_S(s_1) f_S(T_{ij})} \beta_1(T_{ij}) K_h(T_{ij} - t) \{(T_{ij} - t)/h\}^r \right] \\
 &= \bar{m}_y \int_{\mathcal{T}} \mathcal{Q}(s_1, x) K_{h_R}(s_2 - x) \beta_1(x) K_h(x - t) \{(x - t)/h\}^r dx, \\
 &= \bar{m}_y \int_{\mathcal{T}} \mathcal{Q}(s_1, u h_R + s_2) K(u) \beta_1(u h_R + s_2) K_h(u h_R + s_2 - t) \{(u h_R + s_2 - t)/h\}^r du \\
 &= \bar{m}_y \int_{\mathcal{T}} \mathcal{Q}(s_1, s_2) \beta_1(s_2) K(u) K_h(u h_R + s_2 - t) \{(u h_R + s_2 - t)/h\}^r du \{1 + o(1)\} \\
 &= \bar{m}_y \mathcal{Q}(s_1, s_2) \beta_1(s_2) K_h(s_2 - t) \left\{ \frac{s_2 - t}{h} \right\}^r \{1 + o(1)\},
 \end{aligned}$$

where the last equation is due to assumption $h_R/h = o(1)$ in Condition (C.7). Define

$$\mathcal{A}_1^\dagger(s_1, s_2) = \bar{m}_y \mathcal{Q}(s_1, s_2) \beta_1(s_2), \quad (\text{A.19})$$

then

$$\begin{aligned}
 R_{r,31}^*(t) &= \left\{ \frac{1}{n} \sum_{i'=1}^n \frac{1}{M_{x,i'}} \sum_{l \neq l'} u_{i',ll'}^* \mathcal{A}_1^\dagger(S_{i'l}, S_{i'l'}) K_h(S_{i'l'} - t) \left(\frac{S_{i'l'} - t}{h} \right)^r \right\} \{1 + o_p(1)\} \\
 &= O_p\{(nh)^{-1/2}\}
 \end{aligned} \quad (\text{A.20})$$

for both $r = 0$ and 1 . Next, similar to (A.11),

$$\begin{aligned}
 R_{r,32}^*(t) &= \left[\frac{1}{n} \sum_{i=1}^n \left\{ \boldsymbol{\Psi}_{*i} \left(\hat{\boldsymbol{\Lambda}} - \boldsymbol{\Lambda} \right) \boldsymbol{\Psi}_i^T \boldsymbol{\Sigma}_i^{-1} \mathbf{W}_i \right\}^T \mathbf{K}_{r,*i}(t) \boldsymbol{\beta}_{*i} \tilde{\mathbf{X}}_{*i} \right] \{1 + o_p(1)\} \\
 &= \left[\frac{1}{n} \sum_{i=1}^n \mathbf{W}_i^T \boldsymbol{\Sigma}_i^{-1} \boldsymbol{\Psi}_i \left\{ \frac{1}{n} \sum_{i'=1}^n \frac{1}{M_{x,i'}} \sum_{l \neq l'} u_{i',ll'}^* \mathbf{A}_2(S_{i'l}, S_{i'l'}) \right\} \boldsymbol{\Psi}_{*i}^T \mathbf{K}_{r,*i}(t) \boldsymbol{\beta}_{*i} \tilde{\mathbf{X}}_{*i} \right] \\
 &\quad \times \{1 + o_p(1)\} \\
 &= \left[\frac{1}{n} \sum_{i'=1}^n \frac{1}{M_{x,i'}} \sum_{l' \neq l} u_{i',ll'}^* \left\{ \frac{1}{n} \sum_{i=1}^n \mathbf{W}_i^T \boldsymbol{\Sigma}_i^{-1} \boldsymbol{\Psi}_i \mathbf{A}_2(S_{i'l}, S_{i'l'}) \boldsymbol{\Psi}_{*i}^T \mathbf{K}_{r,*i}(t) \boldsymbol{\beta}_{*i} \tilde{\mathbf{X}}_{*i} \right\} \right] \\
 &\quad \times \{1 + o_p(1)\}.
 \end{aligned}$$

Define

$$\mathcal{A}_2^\dagger(s_1, s_2, t) = \bar{m}_y f_T(t) \beta_1(t) \boldsymbol{\psi}^T(t) \boldsymbol{\Lambda} \mathbb{E} \left(\boldsymbol{\Psi}_i^T \boldsymbol{\Sigma}_i^{-1} \boldsymbol{\Psi}_i \right) \mathbf{A}_2(s_1, s_2) \boldsymbol{\psi}(t), \quad (\text{A.21})$$

then it follows that

$$\begin{aligned}
 &\mathbb{E} \left\{ \mathbf{W}_i^T \boldsymbol{\Sigma}_i^{-1} \boldsymbol{\Psi}_i \mathbf{A}_2(s_1, s_2) \boldsymbol{\Psi}_{*i}^T \mathbf{K}_{0,*i}(t) \boldsymbol{\beta}_{*i} \tilde{\mathbf{X}}_{*i} \right\} \\
 &= \text{tr} \left\{ \boldsymbol{\Lambda} \mathbb{E} \left(\boldsymbol{\Psi}_i^T \boldsymbol{\Sigma}_i^{-1} \boldsymbol{\Psi}_i \right) \mathbf{A}_2(s_1, s_2) \mathbb{E} \left(\boldsymbol{\Psi}_{*i}^T \mathbf{K}_{0,*i}(t) \boldsymbol{\beta}_{*i} \boldsymbol{\Psi}_{*i} \right) \right\} \\
 &= \mathcal{A}_2^\dagger(s_1, s_2, t) + O(h^2),
 \end{aligned}$$

and therefore

$$R_{0,32}^*(t) = \left[\frac{1}{n} \sum_{i'=1}^n \frac{1}{M_{x,i'}} \sum_{l' \neq l} u_{i',l'}^* \mathcal{A}_2^\dagger(S_{i'l}, S_{i'l'}, t) \right] \{1 + o_p(1)\} = O_p(n^{-1/2}). \quad (\text{A.22})$$

Using similar derivations we can prove that $R_{1,32}^*(t) = O_p[\{h + (nh)^{-1/2}\}n^{-1/2}]$.

Next, similarly

$$\begin{aligned} R_{r,33}^*(t) &= \left[\frac{1}{n} \sum_{i=1}^n \left\{ \Psi_{*i} \Lambda \left(\widehat{\Psi}_i - \Psi \right)^\top \Sigma_i^{-1} \mathbf{W}_i \right\}^\top \mathbf{K}_{r,*i}(t) \beta_{*i} \widetilde{\mathbf{X}}_{*i} \right] \{1 + o_p(1)\} \\ &= \left[\frac{1}{n} \sum_{i=1}^n \mathbf{W}_i^\top \Sigma_i^{-1} \left\{ \frac{1}{n} \sum_{i'=1}^n \frac{1}{M_{x,i'}} \sum_{l' \neq l} u_{i',l'}^* \mathbf{A}_1(S_{i'l}, S_{i'l'}, \mathbf{S}_i) \right\} \Lambda \Psi_{*i}^\top \mathbf{K}_{r,*i}(t) \beta_{*i} \widetilde{\mathbf{X}}_{*i} \right] \\ &\quad \times \{1 + o_p(1)\} \\ &= \left[\frac{1}{n} \sum_{i'=1}^n \frac{1}{M_{x,i'}} \sum_{l' \neq l} u_{i',l'}^* \left\{ \frac{1}{n} \sum_{i=1}^n \mathbf{W}_i^\top \Sigma_i^{-1} f_S^{-1}(S_{i'l}) \mathbf{K}_i^\dagger(S_{i'l'}, \mathbf{S}_i) \boldsymbol{\psi}(S_{i'l})^\top \Psi_{*i}^\top \right. \right. \\ &\quad \left. \left. \times \mathbf{K}_{r,*i}(t) \beta_{*i} \widetilde{\mathbf{X}}_{*i} \right\} + O_p(n^{-1/2}) \right] \times \{1 + o_p(1)\}. \end{aligned}$$

Denote by $\sigma_i^{(j,j')}$ the (j, j') -th entry of Σ_i^{-1} , and define

$$\begin{aligned} \mathcal{A}_3^\dagger(s_1, s_2, t) &= \frac{\bar{m}_y \beta_1(t) f_T(t)}{f_S(s_1)} \boldsymbol{\psi}(s_1)^\top \boldsymbol{\psi}(t) \sum_{k=1}^q \omega_k \psi_k(t) \\ &\quad \times \mathbb{E} \left[\sum_{j=1}^{m_{x,i}} \sum_{j'=1}^{m_{x,i}} \mathbb{E} \left\{ \psi_k(S_{ij}) \sigma_i^{(j,j')} \mid S_{ij'} = s_2 \right\} \right], \quad (\text{A.23}) \end{aligned}$$

then

$$\begin{aligned} &\mathbb{E} \{ \mathbf{W}_i^\top \Sigma_i^{-1} f_S^{-1}(s_1) \mathbf{K}_i^\dagger(s_2, \mathbf{S}_i) \boldsymbol{\psi}(s_1)^\top \Psi_{*i}^\top \mathbf{K}_{0,*i}(t) \beta_{*i} \widetilde{\mathbf{X}}_{*i} \} \\ &= f_S^{-1}(s_1) \text{tr} \left[\mathbb{E} \left\{ \Lambda \Psi_i^\top \Sigma_i^{-1} \mathbf{K}_i^\dagger(s_2, \mathbf{S}_i) \boldsymbol{\psi}(s_1)^\top \Psi_{*i}^\top \mathbf{K}_{0,*i}(t) \beta_{*i} \Psi_{*i} \right\} \right] \\ &= \bar{m}_y \beta_1(t) f_T(t) f_S^{-1}(s_1) \text{tr} \left[\mathbb{E} \left\{ \Lambda \Psi_i^\top \Sigma_i^{-1} \mathbf{K}_i^\dagger(s_2, \mathbf{S}_i) \boldsymbol{\psi}(s_1)^\top \boldsymbol{\psi}(t) \boldsymbol{\psi}^\top(t) \right\} \right] + O(h^2) \\ &= \bar{m}_y \boldsymbol{\psi}(s_1)^\top \boldsymbol{\psi}(t) \beta_1(t) f_T(t) f_S^{-1}(s_1) \mathbb{E} \left\{ \boldsymbol{\psi}^\top(t) \Lambda \Psi_i^\top \Sigma_i^{-1} \mathbf{K}_i^\dagger(s_2, \mathbf{S}_i) \right\} + O(h^2) \\ &= \mathcal{A}_3^\dagger(s_1, s_2, t) + O(h_R^2) + O(h^2). \end{aligned}$$

Therefore

$$R_{0,33}^*(t) = \left[\frac{1}{n} \sum_{i'=1}^n \frac{1}{M_{x,i'}} \sum_{l' \neq l} u_{i',l'}^* \mathcal{A}_3^\dagger(S_{i'l}, S_{i'l'}, t) \right] \{1 + o_p(1)\} = O_p(n^{-1/2}), \quad (\text{A.24})$$

and following the same line of derivation we can show $R_{1,33}^*(t) = O_p[\{h + (nh_R^2)^{-1/2}\}n^{-1/2}]$.

Using similar but lengthier derivations,

$$\begin{aligned}
 R_{r,34}^*(t) &= \left[\frac{1}{n} \sum_{i=1}^n \left\{ \Psi_{*i} \Lambda \Psi_i^T \Sigma_i^{-1} (\Sigma_i - \widehat{\Sigma}_i) \Sigma_i^{-1} \mathbf{W}_i \right\}^T \mathbf{K}_{r,*i}(t) \beta_{*i} \widetilde{\mathbf{X}}_{*i} \right] \{1 + o_p(1)\} \\
 &= - \left\{ \frac{1}{n} \sum_{i=1}^n \left[\mathbf{W}_i^T \Sigma_i^{-1} \left\{ (\widehat{\Psi}_i - \Psi_i) \Lambda \Psi_i^T + \Psi_i (\widehat{\Lambda} - \Lambda) \Psi_i^T + \Psi_i \Lambda (\widehat{\Psi}_i - \Psi_i)^T \right\} \right. \right. \\
 &\quad \left. \left. \times \Sigma_i^{-1} \Psi_i \Lambda \Psi_{*i}^T \mathbf{K}_{r,*i}(t) \beta_{*i} \widetilde{\mathbf{X}}_{*i} \right] \right\} \{1 + o_p(1)\} \\
 &= \begin{cases} O_p(n^{-1/2}), & \text{if } r = 0, \\ O_p[\{h + (nh_R^2)^{-1/2}\} n^{-1/2}], & \text{if } r = 1. \end{cases} \quad (\text{A.25})
 \end{aligned}$$

Combining (A.20), (A.22), (A.24) and (A.25), we obtain that

$$R_{0,3}^*(t) = - \left\{ \frac{1}{n} \sum_{i'=1}^n \frac{1}{M_{x,i'}} \sum_{l \neq l'} u_{i',ll'}^* \mathcal{A}_1^\dagger(S_{i'l}, S_{i'l'}) K_h(S_{i'l'} - t) \right\} \{1 + o_p(1)\}, \quad (\text{A.26})$$

and $R_{1,3}^*(t) = O_p\{(nh)^{-1/2}\}$. Combining the derivations above, we have

$$\begin{aligned}
 \widehat{\beta}_1(t) - \beta_1(t) &= R_0^*(t)/S_0(t) \times \{1 + O_p(h^2)\} + O_p\{h \times (nh)^{-1/2}\} \\
 &= \frac{1}{2} \beta_1^{(2)}(t) \sigma_K^2 h^2 + \frac{1}{n \bar{m}_y f_T(t) \Gamma_x(t)} \sum_{i=1}^n (\mathcal{Z}_{i1} + \mathcal{Z}_{i2} + \mathcal{Z}_{i3}) + o_p\{(nh)^{-1/2}\},
 \end{aligned} \quad (\text{A.27})$$

where

$$\begin{aligned}
 \mathcal{Z}_{i1} &= \sum_{j=1}^{m_{y,i}} \widetilde{X}_i(T_{ij}) \epsilon_i(T_{ij}) K_h(T_{ij} - t), \\
 \mathcal{Z}_{i2} &= \sum_{j=1}^{m_{y,i}} \widetilde{X}_i(T_{ij}) \beta_1(T_{ij}) \{X_i(T_{ij}) - \widetilde{X}_i(T_{ij})\} K_h(T_{ij} - t), \\
 \mathcal{Z}_{i3} &= - \frac{\bar{m}_y}{M_{x,i}} \sum_{l \neq l'} u_{i,ll'}^* \mathcal{Q}(S_{il}, S_{il'}) \beta_1(S_{il'}) K_h(S_{il'} - t).
 \end{aligned}$$

As \mathcal{Z}_{i1} , \mathcal{Z}_{i2} and \mathcal{Z}_{i3} are independent, zero-mean variables, straightforward calculations show

$$\begin{aligned}
 \mathbb{E}(\mathcal{Z}_{i1}^2) &= h^{-1} \bar{m}_y \Gamma_x(t) \Omega(t, t) f_T(t) \nu_0 + o(h^{-1}) := h^{-1} \Gamma_1(t) + o(h^{-1}), \\
 \mathbb{E}(\mathcal{Z}_{i2}^2) &= h^{-1} \beta_1^2(t) \bar{m}_y \mathbb{E}[\widetilde{X}^2(t) \{X(t) - \widetilde{X}(t)\}^2] \nu_0 + o(h^{-1}) := h^{-1} \beta_1^2(t) \Gamma_2(t) + o(h^{-1}), \\
 \mathbb{E}(\mathcal{Z}_{i3}^2) &= h^{-1} \beta_1^2(t) \bar{m}_y^2 f_S(t) \nu_0 \left[\mathbb{E}(M_{x,i}^{-1}) \int \Pi(t, s_2, s_2) \mathcal{Q}^2(s_2, t) f_S(s_2) ds_2 \right. \\
 &\quad \left. + \mathbb{E}\{M_{x,i}^{-1}(m_{x,i} - 2)\} \int \Pi(t, s_2, s_3) \mathcal{Q}(s_2, t) \mathcal{Q}(s_3, t) f_S(s_2) f_S(s_3) ds_2 ds_3 \right] \\
 &\quad + o(h^{-1}). \\
 &:= h^{-1} \beta_1^2(t) \Gamma_3(t) + o(h^{-1}),
 \end{aligned}$$

where $\Pi(s_1, s_2, s_3) = E\{X^2(s_1)X(s_2)X(s_3)\} + R(s_2, s_3)\sigma_u^2 - R(s_1, s_2)R(s_1, s_3) + I(s_2 = s_3)\{R(s_1, s_1)\sigma_u^2 + \sigma_u^4\}$. Since $\epsilon_i(\cdot)$ is independent of $X_i(\cdot)$ and \mathbf{W}_i , it follows that $E(\mathcal{Z}_{i1}\mathcal{Z}_{i2}) = 0$, and $E(\mathcal{Z}_{i1}\mathcal{Z}_{i3}) = 0$. We can also show $E(\mathcal{Z}_{i2}\mathcal{Z}_{i3}) = O(1) = o_p(h^{-1})$. Therefore, we conclude \mathcal{Z}_{i1} , \mathcal{Z}_{i2} and \mathcal{Z}_{i3} are asymptotically independent. The theorem is proven by applying the central limit theorem to (A.27).

Appendix B: An Extension to Multiple Asynchronous Time-Varying Covariates

B.1 Multiple Asynchronous Covariates

The functional calibration method can be easily extended to accommodate multiple time-varying covariates, which are asynchronous with the response. Our strategy is to apply the multivariate functional principal component analysis (Chiou et al., 2014) to reconstruct the trajectory for each time-varying covariate, then apply time-varying and time-invariant regression analysis using the imputed covariate values that are synchronized with the response.

Suppose there are p_x asynchronous time-varying covariates $\mathbf{X}_i(t) = (X_{i1}, X_{i2}, \dots, X_{ip_x})^T(t)$. The time-invariant and time-varying regression models (1) and (2) can be generalized to

$$Y_i(t) = \beta_0 + \beta_z^T \mathbf{Z}_i + \beta_x^T \mathbf{X}_i(t) + \epsilon_i(t), \quad (\text{B.1})$$

$$Y_i(t) = \beta_0(t) + \beta_z^T(t) \mathbf{Z}_i + \beta_x^T(t) \mathbf{X}_i(t) + \epsilon_i(t), \quad (\text{B.2})$$

where \mathbf{Z}_i is a p_z -dim time-invariant covariate. Consider $\mathbf{X}_i(t)$ as independent realizations of a multivariate stochastic process with the mean and (cross-)covariance functions as

$$\begin{aligned} \mu_v(t) &= E\{X_{iv}(t)\}, \quad R_v(s, t) = \text{Cov}\{X_{iv}(s), X_{iv}(t)\}, \quad s, t \in \mathcal{T}, \quad v = 1, \dots, p_x; \\ R_{vv'}(s, t) &= \text{Cov}\{X_{iv}(s), X_{iv'}(t)\}, \quad v \neq v'. \end{aligned}$$

The discrete, error-prone observations on the time-varying covariates are

$$W_{iv,j} = X_{iv}(S_{iv,j}) + U_{iv,j}, \quad i = 1, \dots, n, \quad j = 1, \dots, m_{x,iv}, \quad (\text{B.3})$$

where $U_{iv,j}$ are zero mean measurement errors independent of $\mathbf{X}_i(t)$ with variance σ_{uv}^2 . On the other hand, the response $Y_i(t)$ are observed on $\mathbf{T}_i = (T_{i1}, \dots, T_{im_{y,i}})^T$. Under the asynchronous longitudinal design, the observation time points from different variables, \mathbf{T}_i and $\mathbf{S}_{iv} = (S_{iv,1}, \dots, S_{iv,m_{x,iv}})^T$, $v = 1, \dots, p_x$, can be different from each other.

B.2 Multivariate Functional Calibration

We consider each asynchronous, time-varying covariate as a stochastic process with a Karhunen–Loève expansion,

$$X_{iv}(t) = \mu_v(t) + \sum_{k=1}^{q_v} \xi_{iv,k} \psi_{vk}(t), \quad t \in \mathcal{T}, \quad (\text{B.4})$$

for $v = 1, \dots, p_x$, $i = 1, \dots, n$, where the $\xi_{iv,k}$ are the principal component scores with mean zero and variance ω_{vk} , $\psi_{vk}(t)$ are orthonormal functions in the sense $\int_{\mathcal{T}} \psi_{vk}(t) \psi_{vk'}(t) dt = 1$

if $k = k'$ and 0 otherwise. Since different components of $\mathbf{X}_i(t)$ can be correlated, these correlations are modeled by cross-covariates between the principal component scores, $\omega_{vv',kk'} = \text{Cov}(\xi_{iv,k}, \xi_{iv',k'}) = \iint R_{vv'}(s, t) \psi_{vk}(s) \psi_{v'k'}(t) ds dt$, $v, v' = 1, \dots, p_x$, $k \leq q_v$ and $k' \leq q_{v'}$. As discussed in Happ and Greven (2018), the univariate Karhunen–Loève representation used in (B.4) is equivalent to the multivariate representation in Chiou et al. (2014).

As in Section 3.1, we obtain mean, covariance and eigenfunction estimates for each time-varying variable, namely $\hat{\mu}_v$, \hat{R}_v , $\hat{\psi}_{vk}$ for $v = 1, \dots, p_x$, $k = 1, \dots, q_v$. We then estimate the cross covariance function $R_{vv'}(s, t)$ by $\hat{R}_{vv'}(s, t) = \hat{a}_0$ where $(\hat{a}_0, \hat{a}_1, \hat{a}_2)$ minimizes

$$\frac{1}{n} \sum_{i=1}^n \left[\frac{1}{m_{x,iv} m_{x,iv'}} \sum_{j=1}^{m_{x,iv}} \sum_{l=1}^{m_{x,iv'}} \{L_{iv,j} L_{iv',l} - a_0 - a_1(S_{iv,j} - s) - a_2(S_{iv',l} - t)\}^2 \right. \\ \left. \times K_{h_{vv'}}(S_{iv,j} - s) K_{h_{vv'}}(S_{iv',l} - t) \right],$$

where $L_{iv,j} = W_{iv,j} - \hat{\mu}_v(S_{iv,j})$. We then estimate cross covariance of the FPC scores by

$$\hat{\omega}_{vv',kk'} = \int \int \hat{R}_{vv'}(s, t) \hat{\psi}_{vk}(s) \hat{\psi}_{v'k'}(t) ds dt,$$

which is implemented by numerical integration. We follow the multivariate PACE method of Chiou et al. (2014) to estimate the FPCA scores. Let $\boldsymbol{\mu}_{iv} = \{\mu_{iv}(S_{iv,1}), \dots, \mu_{iv}(S_{iv,m_{x,iv}})\}^T$, $\mathbf{W}_{iv} = (W_{iv,1}, \dots, W_{iv,m_{x,iv}})^T$ for $v = 1, \dots, p_x$. Let $\boldsymbol{\omega}_{vv'k} = (\omega_{vv',k1}, \dots, \omega_{vv',kq_{v'}})$, note $\omega_{vv,kk'} = 0$ if $k \neq k'$. Define Ω_v as the matrix containing all eigenvalues related to v ,

$$\Omega_v = \begin{bmatrix} \boldsymbol{\omega}_{v11} & \boldsymbol{\omega}_{v21} & \dots & \boldsymbol{\omega}_{vp_x1} \\ \boldsymbol{\omega}_{v12} & \boldsymbol{\omega}_{v22} & \dots & \boldsymbol{\omega}_{vp_x2} \\ \vdots & \vdots & \ddots & \vdots \\ \boldsymbol{\omega}_{v1q_v} & \boldsymbol{\omega}_{v2q_v} & \dots & \boldsymbol{\omega}_{vp_xq_v} \end{bmatrix}.$$

Put $\boldsymbol{\Psi}_{iv} = (\boldsymbol{\psi}_{iv1}, \dots, \boldsymbol{\psi}_{ivq_v})$, where $\boldsymbol{\psi}_{ivk} = \{\psi_{vk}(S_{iv,1}), \dots, \psi_{vk}(S_{iv,m_{x,iv}})\}^T$ for $k = 1, \dots, q_v$, and define $\boldsymbol{\Psi}_i = \text{diag}(\boldsymbol{\Psi}_{i1}, \dots, \boldsymbol{\Psi}_{ip_x})$ as a diagonal block matrix containing eigenfunctions evaluated at \mathbf{S}_i . Similar to the univariate case (5), the BLUP for $\boldsymbol{\xi}_{iv}$ is

$$\tilde{\boldsymbol{\xi}}_{iv} = (\tilde{\xi}_{iv1}, \dots, \tilde{\xi}_{ivK})^T = \Omega_v \boldsymbol{\Psi}_i^T \boldsymbol{\Sigma}_i^{-1} (\mathbf{W}_i - \boldsymbol{\mu}_i),$$

where $\boldsymbol{\mu}_i = (\boldsymbol{\mu}_{i1}^T, \dots, \boldsymbol{\mu}_{ip_x}^T)^T$, $\mathbf{W}_i = (\mathbf{W}_{i1}^T, \dots, \mathbf{W}_{ip_x}^T)^T$, and $\boldsymbol{\Sigma}_i = (\boldsymbol{\Sigma}_{i,vv'})_{v,v'=1}^{p_x}$ with $\boldsymbol{\Sigma}_{i,vv'} = \text{Cov}(\mathbf{W}_{iv}, \mathbf{W}_{iv'})$. Substituting all unknown functions and parameters with their FPCA estimators, the empirical FPC score estimators are given by

$$\hat{\boldsymbol{\xi}}_{iv} = \hat{\Omega}_v \hat{\boldsymbol{\Psi}}_i^T \hat{\boldsymbol{\Sigma}}_i^{-1} (\mathbf{W}_i - \hat{\boldsymbol{\mu}}_i), \quad (\text{B.5})$$

and we can predict the trajectories of the time-varying covariate processes by

$$\hat{X}_{iv}(t) = \hat{\mu}_v(t) + \sum_{k=1}^{q_v} \hat{\xi}_{iv,k} \hat{\psi}_{vk}(t), \quad t \in \mathcal{T}.$$

We then calibrate the covariate values synchronized with the response, $\hat{\mathbf{X}}_{*ij} = \{\hat{X}_{i1}(T_{ij}), \dots, \hat{X}_{ip_x}(T_{ij})\}^T$, and use them to fit regression models (B.1) and (B.2). Denote $\boldsymbol{\beta} = (\beta_0, \boldsymbol{\beta}_z^T, \boldsymbol{\beta}_x^T)^T$, $\mathbb{X}_{ij} = (1, \mathbf{Z}_i^T, \hat{\mathbf{X}}_{*ij}^T)^T$ and $\mathbb{X}_i = (\mathbb{X}_{i1}, \dots, \mathbb{X}_{im_{y,i}})^T$, then Model (B.1) can be fitted by a least square estimator similar as (12). For Model (B.2), denote $\boldsymbol{\beta}(t) = (\beta_0, \boldsymbol{\beta}_z^T, \boldsymbol{\beta}_x^T)^T(t)$. For any fixed t , denote by $\mathbf{b}_0 = \boldsymbol{\beta}(t)$ and $\mathbf{b}_1 = \boldsymbol{\beta}'(t)$. Then $\boldsymbol{\beta}(t)$ can be estimated by solving a kernel weighted local least square as (13).

Appendix C: Additional Tables and Graphs

Error type	Setting I		Setting II	
	independent	dependent	independent	dependent
Bias	-0.010	0.003	0.007	0.008
SD	0.165	0.189	0.086	0.093
Naive SE	0.112	0.103	0.057	0.052
Naive CP	0.825	0.740	0.800	0.725
Bootstrap SE	0.180	0.187	0.089	0.100
Bootstrap CP	0.965	0.935	0.950	0.950

Table C.1: Simulation 1: the performance of $\hat{\beta}_0$ obtained by the proposed FCAR method under different scenarios, including bias, standard deviation, mean of the naive standard error, coverage rate of a 95% confidence interval using the naive SE, mean of the bootstrap standard error, and coverage rate of a 95% confidence interval using the bootstrap SE.

		Independent error			Dependent error		
		FCAR	KW	LOCF	FCAR	KW	LOCF
Setting I	Bias	-0.010	1.163	4.808	0.003	1.092	4.851
	SD	0.165	0.400	0.274	0.189	0.418	0.304
	SE	0.180	0.300	0.238	0.187	0.315	0.233
	CP	0.965	0.115	0.000	0.935	0.125	0.000
Setting II	Bias	0.007	0.166	0.124	0.008	0.162	0.130
	SD	0.086	0.126	0.098	0.093	0.117	0.111
	SE	0.089	0.121	0.080	0.100	0.126	0.076
	CP	0.950	0.705	0.635	0.950	0.730	0.585

Table C.2: Simulation 1: comparisons of $\hat{\beta}_0$ using the proposed FCAR method with those from the kernel weighted (KW) method of (Cao et al., 2015) and the last-observation-carry-forward (LOCF) method in bias, standard deviation, mean of standard error and coverage rate of a 95% confidence interval using standard error.

FUNCTIONAL CALIBRATION

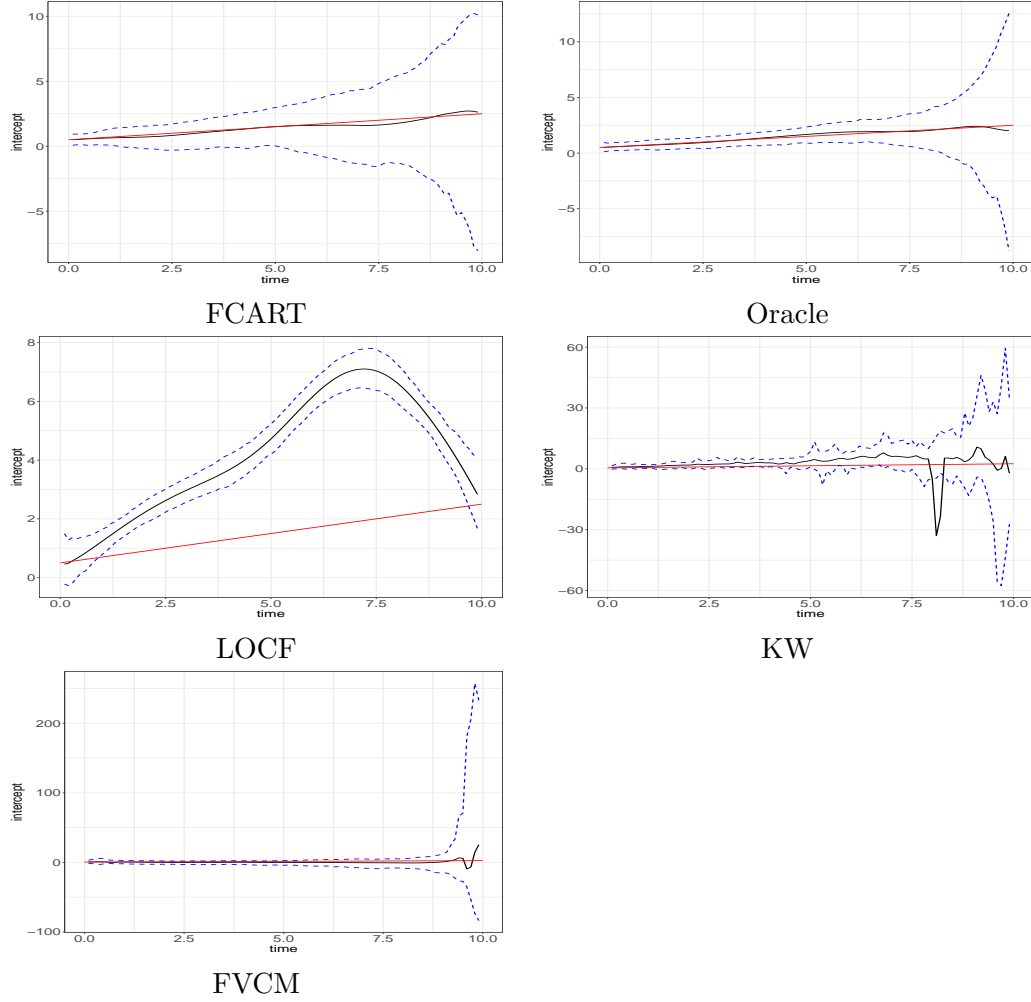


Figure C.1: Summary of $\hat{\beta}_0(t)$ under Setting I of Simulation 2 using various methods. In each panel, black: average of $\hat{\beta}_0(t)$, red: true $\beta_0(t)$, dashed blue: 0.975 and 0.025 quantiles.

FUNCTIONAL CALIBRATION

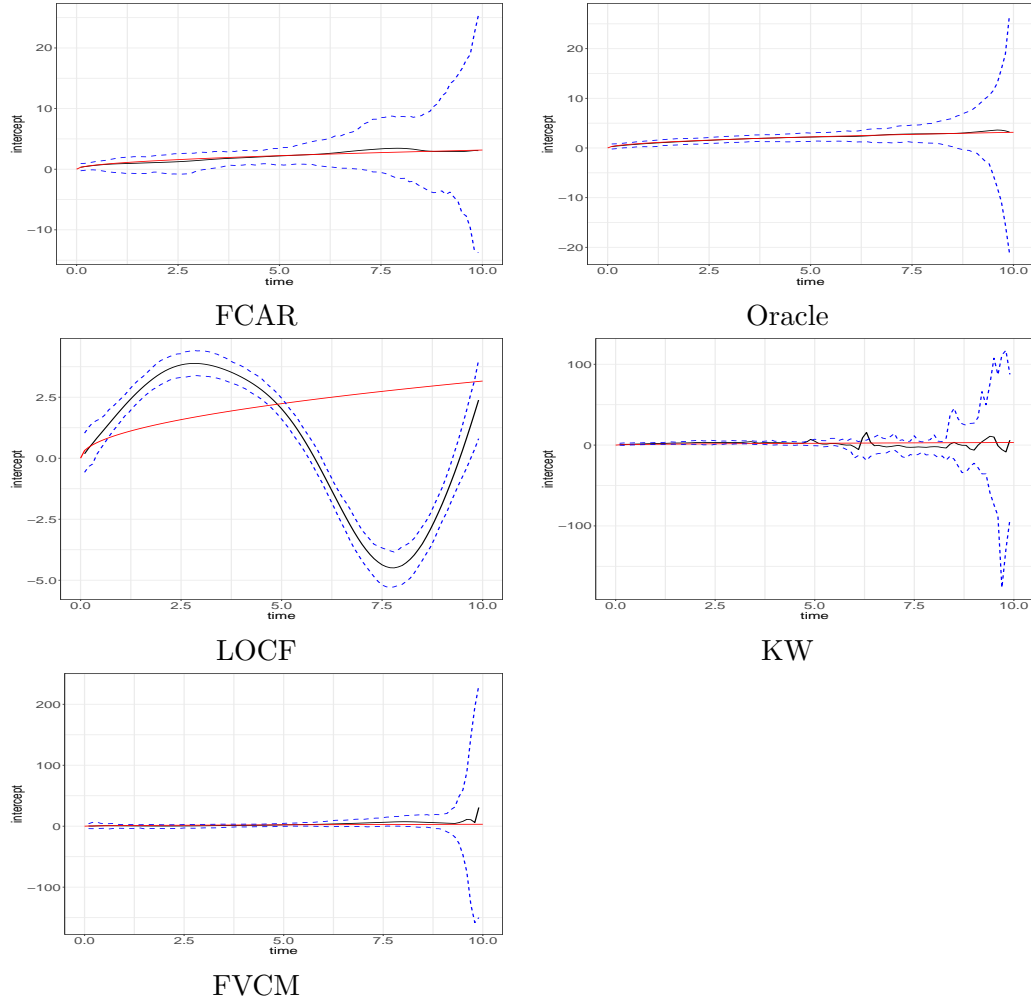


Figure C.2: Summary of $\hat{\beta}_0(t)$ under Setting II of Simulation 2 using various methods. In each panel, black: average of $\hat{\beta}_0(t)$, red: true $\beta_0(t)$, dashed blue: 0.975 and 0.025 quantiles.

FUNCTIONAL CALIBRATION

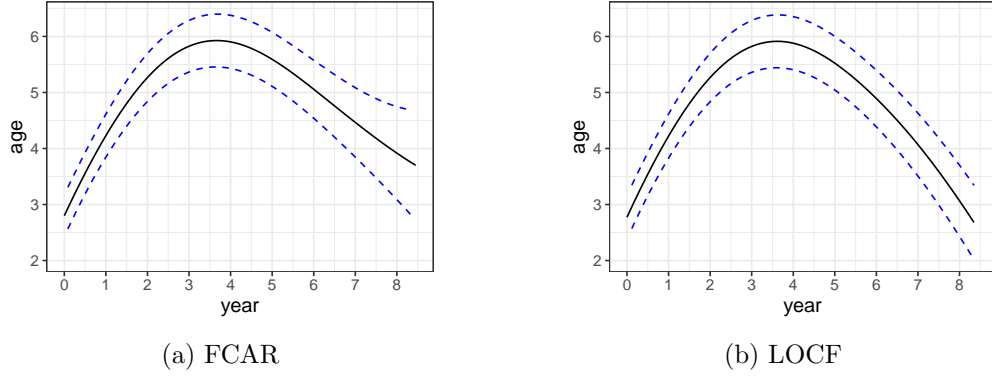


Figure C.3: SWAN data analysis: time-varying coefficient for baseline age estimated using FCAR (left panel) and LOCF (right panel). The solid curve is the estimated coefficient function and the dashed curves are 95% point-wise confidence intervals obtained using bootstrap.

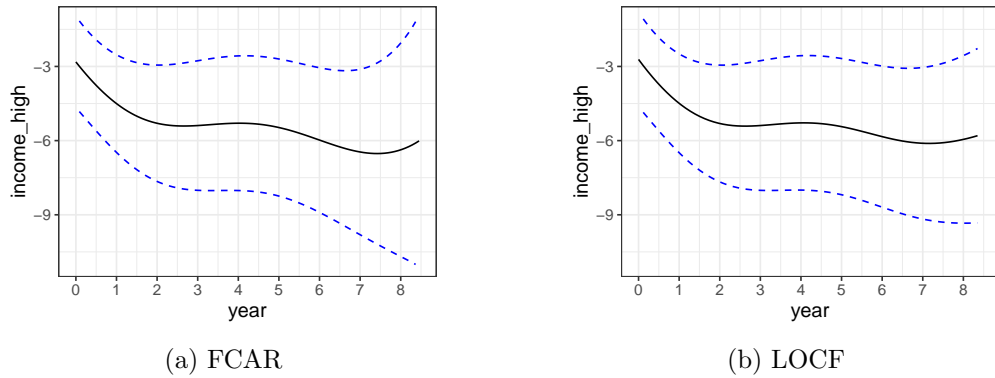


Figure C.4: SWAN data analysis: time-varying coefficient for income level (1: high income; 0: otherwise) estimated using FCAR (left panel) and LOCF (right panel). The solid curve is the estimated coefficient function and the dashed curves are 95% point-wise confidence intervals obtained using bootstrap.